Monte Carlo Calculations of Nuclear Evaporation Processes. III. Applications to Low-Energy Reactions*†

I. DOSTROVSKY AND Z. FRAENKEL, *The Weizmann Institute of Science, Rehovoth, Israel*

AND

G. FRIEDLANDER, *Brookhaven National Laboratory, Upton, New York, and The Weizmann Institute of Science, Rehovoth, Israel*

(Received June 12, 1959)

Monte Carlo calculations of nuclear reactions in the low-energy ($E<50$ Mev) region are described. The calculations are based on the nuclear evaporation model of Weisskopf. Continuum theory was used for the calculation of inverse reaction cross sections. In the calculation of the level densities of excited nuclei, pairing and shell energy corrections were used in terms of characteristic level displacements. The accurate equation rather than the approximate Maxwell distribution was used for the selection of the kinetic energy of the evaporated particle. Experimentally determined Q-values for the various reactions were used. The calculations are compared with experimental measurements for about 60 excitation functions of nuclear reactions in the mass range Cr^{50}–Se^{74}. Cameron's values for pairing energies were used at the outset; but a new set of pairing and shell energy correction values, which leads to substantially improved agreement with the experimental curves, is presented. The procedure which was used to arrive at this set is described and several features of the set are discussed. The need for a further downward correction of the level density of symmetrical ($A=2Z$) nuclei is indicated. Computed excitation functions are shown for all the reactions studied as well as for several reactions for which experimental data are not yet available. Further experiments on reaction cross sections are suggested which would allow a unique determination of the pairing and shell energy corrections of level densities for any value of Z and N in the region under discussion. The existence of a unique set of these correction terms would provide strong evidence for the validity of evaporation theory for the reactions considered.

I. INTRODUCTION

THERE has been a great deal of discussion and controversy about the mechanism of nuclear reactions at moderate energies (<50 Mev), and in particular about the range of validity of the statistical theory on the one hand, and the importance of various direct-interaction mechanisms on the other. In view of the availability of a computer program for Monte Carlo calculations of nuclear evaporation[1] it seemed worthwhile to apply such calculations to nuclei excited to moderate energies; the aim was to establish to what extent and in how much detail the competition between various nuclear reactions and their energy dependence could be fitted by the statistical theory. As it turned out and as will be discussed in Sec. II, the existing Monte Carlo program[1] was rather extensively modified before it was thought to be appropriate for this investigation.

To facilitate a critical test of evaporation theory and a determination of some of the parameters entering the calculations, it was decided to carry out computations in a relatively narrow range of mass numbers in which a large body of experimental data on low-energy nuclear reactions was available. The range $45<A<75$ was chosen because excitation functions of a large number of reaction types with a variety of target nuclides have been studied in this region, and because Coulomb barrier effects in this region of low atomic numbers are sufficiently small to permit substantial competition between charged-particle and neutron emission.

The experimental data with which the calculations are to be compared in the present paper are confined to reaction cross sections although the computations yield the relative numbers and energy spectra of emitted particles also, and these could be compared with corresponding measured quantities. No deuteron-induced reactions were used for comparison because of the known large contribution of stripping mechanisms to these reactions; on the other hand it was deemed important to determine to what extent the excitation functions of reactions induced by helium ions, protons, and neutrons could be accounted for by evaporation theory. The reactions in the mass range of interest, for which suitable experimental excitation function data[2–12] were available to the authors, are listed in Table I.

* Part I of this series (see reference 1) was entitled "Systematics of Nuclear Evaporation." Part II, entitled "A Monte Carlo Calculation of Fission-Spallation Competition," by Dostrovsky, Fraenkel, and Rabinowitz, appeared in the *Proceedings of the Second International Conference on the Peaceful Uses of Atomic Energy, Geneva, 1958* (United Nations, Geneva, 1958), Paper 1615.

† Research performed in part under the auspices of the U. S. Atomic Energy Commission.

[1] Dostrovsky, Rabinowitz, and Bivins, Phys. Rev. **111**, 1659 (1958).

[2] D. O. Raleigh, thesis, Columbia University, 1958 (unpublished); D. O. Raleigh and J. M. Miller (private communication).

[3] R. Chasman and G. Friedlander (unpublished data).

[4] Miller, Friedlander, and Markowitz, Phys. Rev. **98**, 1197 (1955); and Friedlander, Lee, and Miller (unpublished data).

[5] J. Terrell and D. M. Helm, Phys. Rev. **109**, 2031 (1958).

[6] F. S. Houck, Atomic Energy Commission Report NYO-7332, June, 1959 (unpublished); F. S. Houck and J. M. Miller (private communication).

[7] Sharp, Diamond, and Wilkinson, Phys. Rev. **101**, 1493 (1956).

[8] S. N. Ghoshal, Phys. Rev. **80**, 939 (1950).

[9] J. W. Meadows, Phys. Rev. **91**, 885 (1953).

[10] N. T. Porile and D. L. Morrison, Phys. Rev. (to be published).

TABLE I. Experimental excitation function data referred to in this paper.

Target nucleus	Compound nucleus	Reaction[a]	Product	Range of bombarding energies (Mev)	Range of excitation energies (Mev)
$_{22}Ti^{46}$ [b]	$_{24}Cr^{50}$	(α,n)	Cr^{49}	10–27	18–33
		(α,p)	V^{49}	10–27	18–33
		$(\alpha,2n)$	Cr^{48}	22–42	29–47
		(α,pn)	V^{48}	19–42	26–47
		$(\alpha,3n)+(\alpha,p2n)$	V^{47}	30–40	36–45
		$(\alpha,3p)$	Sc^{47}	29–42	35–47
		$(\alpha,\alpha pn)$	Sc^{44}	36–42	42–47
$_{23}V^{50}$ [c]	$_{25}Mn^{54}$	$(\alpha,2n)$	$Mn^{52}+Mn^{52m}$	16–26	24–33
		$(\alpha,2p)$	V^{52}	19–26	27–33
$_{24}Cr^{50}$ [d]	$_{26}Fe^{54}$	$(\alpha,2n)$	Fe^{52}	19–40	26–45
		(α,pn)	$Mn^{52}+Mn^{52m}$	19–40	26–45
$_{26}Fe^{56}$ [e]	$_{26}Fe^{57}$	(n,p)	Mn^{56}	4.4–17.9	12–26
$_{26}Fe^{54}$ [f]	$_{28}Ni^{58}$	(α,n)	Ni^{57}	6.5–40	12–43
		(α,p)	Co^{57}	6.5–40	12–43
		$(\alpha,2n)$	Ni^{56}	17–40	22–43
		(α,pn)	Co^{56}	11–40	17–43
		$(\alpha,p2n)$	Co^{55}	21–40	26–43
		$(\alpha,2pn)$	Fe^{55}	27–40	31–43
$_{27}Co^{59}$ [g]	$_{28}Ni^{60}$	(p,pn)	$Co^{58}+Co^{58m}$	14–51	24–60
		$(p,3n)$	Ni^{57}	22–51	31–60
		$(p,p2n)$	Co^{57}	24–51	33–60
		$(p,p3n)$	Co^{56}	30–51	39–60
		$(p,3pn)$	Mn^{55}	40–51	49–60
		$(p,\alpha pn)$	Mn^{54}	30–51	39–60
$_{28}Ni^{58}$ [f]	$_{30}Zn^{62}$	$(\alpha,\alpha n)$	Ni^{57}	17–40	20–41
		$(\alpha,\alpha p)$	Co^{57}	17–40	20–41
		$(\alpha,\alpha 2n)$	Ni^{56}	31–40	33–41
		$(\alpha,\alpha pn)$	Co^{56}	31–40	33–41
$_{28}Ni^{60}$ [h]	$_{30}Zn^{64}$	(α,n)	Zn^{63}	9–39	13–41
		$(\alpha,2n)$	Zn^{62}	20–39	23–41
		(α,pn)	Cu^{62}	20–39	23–41
$_{29}Cu^{63}$ [i]	$_{30}Zn^{64}$	(p,n)	Zn^{63}	8–40	16–47
		$(p,2n)$	Zn^{62}	15–40	22.5–47
		(p,pn)	Cu^{62}	15–40	22.5–47
		$(p,p2n)$	Cu^{61}	20–50	27.5–57
$_{29}Cu^{63}$ [h]	$_{30}Zn^{64}$	(p,n)	Zn^{63}	5–12	12.5–29
		$(p,2n)$	Zn^{62}	14–32	21.5–40
		(p,pn)	Cu^{62}	14–32	21.5–40
$_{29}Cu^{65}$ [i]	$_{30}Zn^{66}$	(p,pn)	Cu^{64}	10–50	18–58
		$(p,3n)$	Zn^{63}	30–50	38–58
		$(p,4n)$	Zn^{62}	30–50	38–58
		$(p,p3n)$	Cu^{62}	30–50	38–58
$_{29}Cu^{63}$ [j]	$_{31}Ga^{67}$	(α,n)	Ga^{66}	15–30	18–32
		$(\alpha,2n)$	Ga^{65}	21.5–40	24–41
		(α,pn)	Zn^{65}	15–40	18–41
		$(\alpha,\alpha n)$	Cu^{62}	21–40	23–41
$_{29}Cu^{65}$ [j]	$_{31}Ga^{69}$	(α,n)	Ga^{68}	15–40	18–42
		$(\alpha,2n)$	Ga^{67}	15–40	18–42
		$(\alpha,2p)$	Cu^{67}	21–40	24–42
		$(\alpha,3n)$	Ga^{66}	32–40	35–42
		$(\alpha,\alpha n)$	Cu^{64}	24–40	27–42
		$(\alpha,2\alpha)$	Co^{61}	26–40	29–42
$_{30}Zn^{64}$ [k]	$_{32}Ge^{68}$	(α,n)	Ge^{67}	13–40	15–40
		(α,p)	Ga^{67}	13–40	15–40
		$(\alpha,2n)$	Ge^{66}	22–40	23–40
		(α,pn)	Ga^{66}	19–40	20.5–40
		$(\alpha,3n)$	Ge^{65}	34–41	35–41
		$(\alpha,p2n)$	Ga^{65}	27–39	28–39
		$(\alpha,2pn)$	Zn^{65}	26–41	27–41
		$(\alpha,\alpha n)$	Zn^{63}	21–41	22–41
		$(\alpha,\alpha 2n)$	Zn^{62}	30–41	31–41
		$(\alpha,\alpha pn)$	Cu^{62}	25–41	26–41
$_{30}Zn^{70}$ [l]	$_{32}Ge^{74}$	(α,pn)	Ga^{72}	21–41	26–45
		$(\alpha,2p)$	Zn^{72}	26.5–41	31–45
$_{32}Ge^{70}$ [l]	$_{34}Se^{74}$	$(\alpha,2n)$	Se^{72}	21–41	24–43
		(α,pn)	As^{72}	21–41	24–43

[a] The notation for the experimentally observed reactions is intended to indicate the final product only, not a reaction path. For example, a reaction labeled (α,pn) may include (α,pn), (α,np), and (α,d).
[b] From reference 2.
[c] From reference 3.
[d] From reference 4.
[e] From reference 5.
[f] From reference 6.
[g] From reference 7.
[h] From reference 8.
[i] From reference 9.
[j] From reference 10.
[k] From reference 11.
[l] From reference 12.

[11] N. T. Porile, Phys. Rev. **315**, 939 (1959).
[12] S. Amiel, Phys. Rev. **116**, 415 (1959).

II. THE CALCULATION

The evaporation calculations of Dostrovsky, Rabinowitz, and Bivins[1] were designed for application to high initial excitation (>50 Mev) and for determination of the relative abundances of the various types of evaporated particles as well as the abundance distribution of mass numbers of residual nuclei. They were not intended to give detailed information on the final product nuclei nor to be taken very seriously when initial excitations of less than 50 Mev were involved. The expressions for relative particle emission widths [Eqs. (2) and (3) of reference 1] were therefore derived with the approximation that the kinetic energy of an evaporated particle is always small compared to the excitation energy, and with other simplifying assumptions. Thus it was not expected that the computer program of reference 1 (known as Mark II) would be directly applicable to the present problem. Nevertheless, it was used as a starting point, and some of the reaction cross sections listed in Table I were calculated with this program. The agreement with experimental data was found to be generally rather poor (see Table IV for some typical examples, in comparison with later results) and a number of modifications were therefore introduced.

It was felt that the poor results obtained with the Mark II program were probably attributable to several causes, of which the approximations in the equations already mentioned were perhaps not even the most significant. In particular, the effects of nucleon pairing and of shells on level densities have already been shown to be important[6,8,9,13–18] and should be taken into account.

Weisskopf's expression[19] for the probability per unit time for the emission of particle j with kinetic energy between ϵ and $\epsilon+d\epsilon$,

$$P_j(\epsilon)d\epsilon=\gamma_j\sigma\epsilon[W(f)/W(i)]d\epsilon, \qquad (1)$$

was used as a starting point for development of a new computer program suitable for Monte Carlo calculations in the low-energy region of interest. Here $\gamma_j=g_jm_j/\pi^2\hbar^3$, with g_j and m_j the number of spin states and the mass of particle j, respectively; σ is the cross section for the inverse reaction; and $W(f)$ and $W(i)$ are the level densities of the final and initial nuclei at their respective excitation energies.

In order to obtain the total emission probability for particle j by integration of Eq. (1), the three factors which require particular attention are σ, $W(f)$, and the limits of integration. The points in which the present

[13] Harris, Muehlhause, and Thomas, Phys. Rev. **79**, 11 (1950).
[14] E. Belmont and J. M. Miller, Phys. Rev. **95**, 1554 (1954).
[15] C. Block, Phys. Rev. **93**, 1094 (1954).
[16] T. D. Newton, Can. J. Phys. **34**, 804 (1956).
[17] A. G. W. Cameron, Can. J. Phys. **36**, 1040 (1958).
[18] Rosenzweig, Bollinger, Lee, and Schiffer, *Second International Conference on the Peaceful Uses of Atomic Energy, Geneva, 1958* (United Nations, Geneva, 1958), Paper 693.
[19] V. F. Weisskopf, Phys. Rev. **52**, 295 (1937).

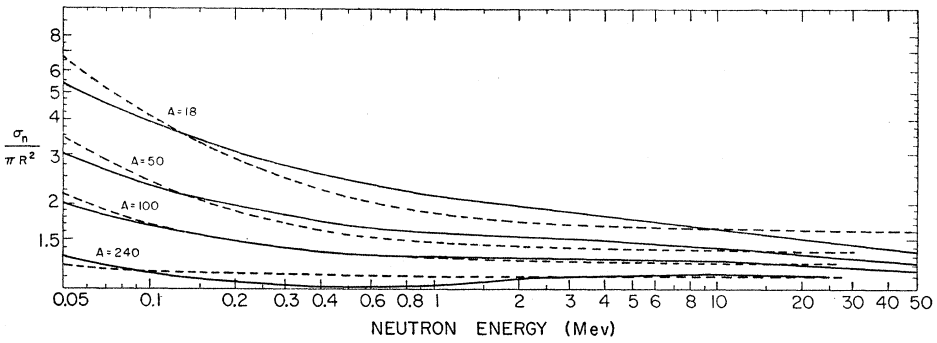

FIG. 1. Neutron capture cross sections as a function of neutron kinetic energy. The ordinate is the ratio of capture cross section to geometric cross section. The solid curves are the continuum-theory cross sections taken from reference 24. The dashed curves are calculated according to Eq. (2).

development of Eq. (1) differs from previous treatments[1,20–23] will now be discussed in detail.

(a) Cross Sections for Inverse Reactions

In the calculations of reference 1 and in most previous treatments, the inverse reaction cross section for neutrons was taken as the geometric cross section of the product nucleus. While this is a good approximation for relatively high neutron energies (of the order of tens of Mev), neutron capture cross sections are known to rise with decreasing energy at lower energies. For the present calculations an attempt was made to approximate the energy and mass number dependence of neutron capture cross sections as given by continuum theory.[24] The empirical equation adopted for this purpose is

$$\sigma_c/\sigma_g=\alpha(1+\beta/\epsilon), \tag{2}$$

where $\alpha=0.76+2.2A^{-\frac{1}{3}}$ and $\beta=(2.12A^{-\frac{2}{3}}-0.050)/(0.76+2.2A^{-\frac{1}{3}})$ Mev, and σ_c and σ_g are the capture and geometric cross sections, respectively. In computing $\sigma_g=\pi R^2$, the nuclear radius was taken as $R=1.5\times10^{-13}A^{\frac{1}{3}}$ cm.

In Fig. 1 neutron cross sections computed by Eq. (2) are compared with those calculated from continuum theory. It is seen that the fit for intermediate nuclei is quite good down to $\epsilon\sim0.05$ Mev. For still lower energies, σ_c according to Eq. (2) tends towards infinity; but since only the product $\sigma_c\epsilon$ enters in Eq. (1), this causes no difficulty. It should be noted, that the inverse cross section needed in Eq. (1) is that between a neutron of kinetic energy ϵ and a nucleus in an excited state. Since little is known about such cross sections, the ground-state cross sections are used as an approximation.

For charged particles, Coulomb barrier effects have to be taken into account in the calculation of the inverse cross sections. The proper quantum mechanical expressions for barrier penetration are far too complex to be used in Eq. (1) if one wishes to retain the equation in an integrable form. In most previous evaporation calculations the barrier effect has been approximately taken into account by multiplying the geometric cross section by the factor $(1-k_jV_j/\epsilon)$, where V_j is the Coulomb barrier for particle j calculated from electrostatics and k_j is a coefficient designed to reproduce barrier penetration approximately. For a given nucleus, values of k_j can be found which lead to a good representation of the barrier effect with this formulation; however, for different values of Z, different values of k_j are needed for a good fit. Most workers have ignored this fact and have used for all values of Z the values of k_j derived by Le Couteur[20] for nuclear-emulsion nuclei ($Z\sim40$) from a general formulation of effective barrier heights by Konopinski and Bethe.[25]

In the present work, the variation of charged-particle capture cross sections with Z and ϵ was approximated by an empirical formula of the following form:

$$\sigma_c/\sigma_g=(1+c_j)(1-k_jV_j/\epsilon). \tag{3}$$

For protons, deuterons, and alpha particles, the constants c_j and k_j were chosen to give a good fit to the continuum-theory cross sections calculated by Shapiro[26] and Blatt and Weisskopf.[24] The values of c_p, k_p, c_α, and k_α are listed in Table II for several values of Z. It turned out that, at all values of Z, c_d can be taken as $c_p/2$ and k_d as $k_p+0.06$. By analogy, it was assumed that $c_{H^3}=c_p/3$ and $k_{H^3}=k_p+0.12$, and that $c_{He^3}=\frac{4}{3}c_\alpha$ and $k_{He^3}=k_\alpha-0.06$. In the energy range of interest here, the emission of H^3 and He^3 is very rare (see

TABLE II. Parameters in Eq. (3) for charged-particle cross sections.

Z	k_p	c_p	k_α	c_α
10	0.42	0.50	0.68	0.10
20	0.58	0.28	0.82	0.10
30	0.68	0.20	0.91	0.10
50	0.77	0.15	0.97	0.08
$\geqslant70$	0.80	0.10	0.98	0.06

[20] K. J. Le Couteur, Proc. Phys. Soc. (London) **A63**, 259 (1950).
[21] Y. Fujimoto and Y. Yamaguchi, Progr. Theoret. Phys. (Kyoto) **4**, 468 (1949); **5**, 787 (1950).
[22] J. W. Meadows, Phys. Rev. **98**, 744 (1955).
[23] G. Rudstam, thesis, University of Uppsala, Uppsala, Sweden, 1956 (unpublished).
[24] J. Blatt and V. F. Weisskopf, *Theoretical Nuclear Physics* (John Wiley & Sons, Inc., New York, 1952).
[25] E. J. Konopinski and H. A. Bethe, Phys. Rev. **54**, 130 (1938).
[26] M. M. Shapiro, Phys. Rev. **90**, 171 (1953).

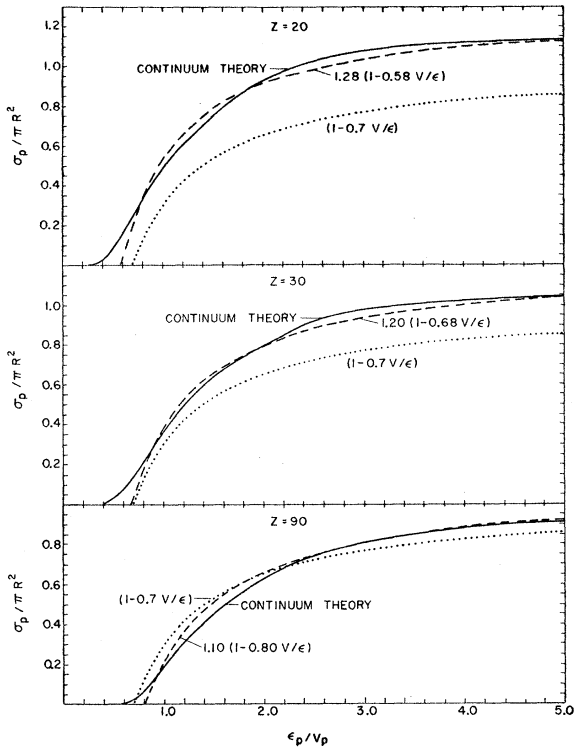

FIG. 2. Proton capture cross sections for three values of Z. The ratio of proton capture cross section to geometric cross section of the capturing nucleus is plotted against the ratio of proton kinetic energy to barrier height. The solid curves represent the continuum-theory cross sections from references 24 and 26. The dashed curves are calculated according to Eq. (3), with the constants of Table II, the dotted curves represent the expression $\sigma_p/\pi R^2=1-0.7V_p/\epsilon_p$ used in previous evaporation calculations.

Table IX), and the actual choice of k and c values for these particles is therefore not very important. In Fig. 2 cross sections for protons as calculated by Eq. (3) are compared with Shapiro's continuum-theory cross sections and also with the approximation used in reference 1 and by other workers.[20,23] Between the Z values listed in Table II, linear interpolation was used for both k_j and c_j.

The classical barrier V_j was calculated with the formula

$$V_j=\frac{zZe^2}{r_0A^{\frac{1}{3}}+\rho_j}, \tag{4}$$

where z and Z are the atomic numbers of the outgoing particle and residual nucleus, and e is the electron charge; r_0 was taken as 1.5×10^{-13} cm. Following Blatt and Weisskopf,[24] ρ_j was taken as 1.2×10^{-13} cm for deuterons and alpha particles, and zero for protons. For H^3 and He^3, ρ_j was assumed to be 1.2×10^{-13} cm also.

It is clear that, at very high energies ($\epsilon/k_jV_j\gg1$), the cross section for particle j calculated with Eq. (3) tends to an asymptotic value $(1+c_j)\sigma_g$, which cannot be correct. This effect is quite unimportant because particles of such high energies are emitted extremely infrequently. As is seen in Fig. 2, the fit to continuum theory is excellent for protons up to $\epsilon_p/V_p\sim5$; it is equally good for deuterons and alpha particles.

The particular form of the energy dependence in Eqs. (2) and (3) was chosen, in preference to others which would give equally good or better fits, in order to preserve Eq. (1) in integrable form.

(b) Level Density

Many different expressions have been proposed[16,17,19,27,28] for the variation of the nuclear level density $W(E)$ with excitation energy E. Those based on the Fermi gas model have in common an exponential term with an exponent proportional to $E^{\frac{1}{2}}$. The simplest and most widely used formulation is that given by Weisskopf[19] for a completely degenerate Fermi gas:

$$W(E)=C\exp[2(aE)^{\frac{1}{2}}]. \tag{5}$$

In more refined treatments[16,17,27,28] C is a function of E, and some authors have also used more complicated terms in the exponential. The use of these more complex expressions in Eq. (1) makes integration in closed form impossible. Approximate integrations after series expansion are possible, and this is the approach used, for example, by Le Couteur[20]; but for residual excitation energies below approximately 1 Mev such expansions are not useful because the series obtained then diverge. Since, at energies above 1 Mev, the energy dependence of C in Eq. (5) introduces only very small effects in the relative emission probabilities of various particles (because of the dominant effect of the exponential term), it was decided to use the simple form of Eq. (5) in the present calculations (with some modifications to be discussed presently). The value of the constant C does not need to be specified, since only ratios of level densities enter Eq. (1) and, over the narrow range of A involved in a single evaporation step, the variation of C with A can be neglected.

As in reference 1, the level density parameter a has again been taken as almost proportional to A,[29] with various values of the proportionality constant. Most calculations were performed with $a=A/20$, which appeared to give the best fit to the experimental data

[27] H. A. Bethe, Revs. Modern Phys. **9**, 69 (1937).
[28] J. M. B. Lang and K. J. Le Couteur, Proc. Phys. Soc. (London) **A67**, 586 (1954).
[29] As in reference 1, Le Couteur's formulation[20] of the slight dependence of the level density parameter a on the neutron excess of the nucleus has been used, *viz.*:

$$a_n=a(1-1.3\theta/A)^2,\quad a_t=a(1-1/A-1.3\theta/A)^2,$$
$$a_p=a(1+1.3\theta/A)^2,\quad a_{He^3}=a(1-1/A+1.3\theta/A)^2,$$
$$a_d=a(1-1/2A)^2,\quad a_\alpha=a(1-3/2A)^2,$$

where $\theta=(N-Z)/A$, and A, Z, N refer to the initial nucleus in an evaporation step; a_n, a_p, etc., are the level density parameters of the product nuclei resulting from evaporation of a neutron, proton, etc., and a is taken proportional to $A-1$. In the range of interest, actual tests showed this isotopic number dependence, which arises from the difference in the Fermi energies for neutrons and protons, to have negligible effects on the evaporation calculations.

(see Sec. IIIa below). Since the present work deals with a rather narrow range of target mass numbers, the proportionality of a and A cannot be considered to be proven by the present calculations.

Nuclear energy level densities depend not only on the total number of nucleons in a nucleus but also on whether the neutron and proton numbers are odd or even.[9,16,17,30,31] As will be shown below, agreement of the results of evaporation calculations with experimental reaction yields could not be obtained if this effect was neglected. Weisskopf and Ewing[30] suggested that the odd-even effect be taken into account in the pre-exponential constant C by setting $C_{\text{odd-odd}}=4C_{\text{even-even}}$ and $C_{\text{even-odd}}=C_{\text{odd-even}}=2C_{\text{even-even}}$ Hurwitz and Bethe[31] pointed out that it is more nearly correct to consider the odd-even effects on level densities as arising from the displacements of ground-state energies caused by nucleon pairing. On this basis they suggest that, for all but odd-odd nuclei, the excitation energy appearing in the level density formula be counted from a corrected ground state or characteristic level, displaced upward from the true ground state. This approach was adopted in the present work and Eq. (5) then becomes

$$W(E)=C\exp\{2[a(E-\delta)]^{\frac{1}{2}}\}, \tag{6}$$

where $\delta=0$ for odd-odd nuclei and $\delta\geqslant 0$ for all other types. The values of δ may be expected to be the pairing energies for neutrons and protons.[32] Cameron[17] has recently tabulated pairing energies for all even values of Z and N as derived from a comparison of his semiempirical mass equation with measured atomic masses. In even-even nuclei the pairing energies of neutrons and protons were considered to be additive.

At and near closed shells, additional level density irregularities are expected.[15,18] Newton[16] has suggested taking shell effects into account in a manner which essentially leads to a characteristic value of a for each neutron and proton number. This formulation was actually incorporated in the computer program at one time; but it was found that, with the parameters given by Newton, the results obtained did not give very good agreement with experimental cross sections; with the large number of parameters available in this formulation it was not thought profitable to attempt to achieve agreement by parameter fitting. The even more elaborate treatment of shell effects by Cameron[17] was also rejected for the present purpose, because it would have required an exorbitant amount of computer time. The scheme finally adopted was to include shell effects in the same manner as the pairing effect, i.e., by an additional δ term in Eq. (6) for closed-shell nuclei. A disadvantage of this procedure is that, as used in the present computer program, it does not permit inclusion of negative δ values which might be appropriate just after closed shells. Positive δ's for shell effects at odd nucleon numbers near closed shells could be included, but were omitted in order to minimize the number of adjustable parameters.

[30] V. F. Weisskopf and D. H. Ewing, Phys. Rev. **57**, 472 (1940).
[31] H. Hurwitz and H. A. Bethe, Phys. Rev. **81**, 898 (1951).
[32] See, e.g., M. El-Nadi and M. Wafik, Nuclear Phys. **9**, 22 (1958).

(c) Computation of Particle Emission Probabilities

With the inverse cross section as given by Eqs. (2) and (3) and the level density as given by Eq. (6) included in Eq. (1), the following equation is obtained for neutron emission:

$$P_n(\epsilon)d\epsilon=g_n\frac{m_n r_0^2 A_n^{\frac{2}{3}}}{\pi\hbar^3}\exp\{-2[a_0(E-\delta_0)]^{\frac{1}{2}}\}\epsilon\alpha\left(1+\frac{\beta}{\epsilon}\right)\times\exp\{2[a_n(E-Q_n-\delta_n-\epsilon)]^{\frac{1}{2}}\}d\epsilon, \tag{7}$$

where the subscripts 0 and n refer to the original and residual nucleus, respectively, and Q_n is the neutron separation energy. It is seen from Eq. (7) that, with the introduction of the pairing and shell correction δ, it is implicitly assumed that the maximum energy available for the evaporation process (i.e., the maximum kinetic energy of the outgoing neutron) is given by

$$(\epsilon_n)_{\max}=E-Q_n-\delta_n. \tag{8}$$

This is, of course, not strictly true. However, the number of energy levels below an excitation energy $E_n=\delta_n$ of the residual nucleus is presumably small, and hence the probability that the evaporation process will lead to levels in this interval is expected to be small. The error introduced with the approximation (8) will therefore in general be small. There exists however one important exception: If neutron emission is the only process energetically possible for de-excitation (except for γ radiation) and the excitation energy of the residual nucleus is in the interval $0\leqslant E_n<\delta_n$, Eq. (8) clearly does not hold, since there is at least one energy level available for the evaporation process—the ground state of the residual nucleus. It will later be shown that this fact indeed introduces an upward shift of the threshold and consequent distortion of the calculated excitation curve. The amount of this distortion will depend, of course, on the density of levels below the characteristic level of the product nucleus in question.

With the approximation (8) the integral of Eq. (7) which gives the total neutron emission width takes the following form:

$$\Gamma_n=g_n\frac{m_n r_0^2 A_n^{\frac{2}{3}}}{\pi\hbar^2}\exp\{-2[a_0(E-\delta_0)]^{\frac{1}{2}}\}\alpha\int_0^{E-Q_n-\delta_n}(\epsilon+\beta)\times\exp\{2[a_n(E-Q_n-\delta_n-\epsilon)]^{\frac{1}{2}}\}d\epsilon. \tag{9}$$

This yields, on integration

$$\Gamma_n=g_n\frac{m_n r_0^2 A_n^{\frac{2}{3}}}{2\pi\hbar^2}\exp\{-2[a_0(E-\delta_0)]^{\frac{1}{2}}\}$$
$$\times\frac{\alpha}{a_n^2}\{a_nR_n[2\exp(2(a_nR_n)^{\frac{1}{2}})+1]$$
$$-(3-2a_n\beta)(a_nR_n)^{\frac{1}{2}}\exp[2(a_nR_n)^{\frac{1}{2}}]$$
$$-\tfrac{1}{2}(3-2a_n\beta)[1-\exp(2(a_nR_n)^{\frac{1}{2}})]\},\quad(10)$$

with

$$R_n=E-Q_n-\delta_n.\quad(11)$$

Since the kinetic energy of a charged particle j cannot be smaller than the effective Coulomb barrier energy k_jV_j, the equation for the charged-particle emission width has the following form:

$$\Gamma_j=g_j\frac{m_j r_0^2 A_j^{\frac{2}{3}}}{\pi\hbar^2}\exp\{-2[a_0(E-\delta_0)]^{\frac{1}{2}}\}$$
$$\times(1+c_j)\int_{k_jV_j}^{E-Q_j-\delta_j}(\epsilon-k_jV_j)$$
$$\times\exp\{2[a_j(E-Q_j-\delta_j-\epsilon)]^{\frac{1}{2}}\}d\epsilon,\quad(12)$$

which yields

$$\Gamma_j=g_j\frac{m_j r_0^2 A_j^{\frac{2}{3}}}{2\pi\hbar^2}\exp\{-2[a_0(E-\delta_0)]^{\frac{1}{2}}\}\frac{(1+c_j)}{a_j^2}$$
$$\times\{a_jR_j[2\exp(2(a_jR_j)^{\frac{1}{2}})+1]$$
$$-3(a_jR_j)^{\frac{1}{2}}\exp[2(a_jR_j)^{\frac{1}{2}}]$$
$$-\tfrac{3}{2}[1-\exp(2(a_jR_j)^{\frac{1}{2}})]\},\quad(13)$$

where

$$R_j=E-Q_j-k_jV_j-\delta_j.\quad(14)$$

Since R_n and R_j, the maximum possible values of the kinetic energies of the emitted neutron or charged particle, respectively, will hardly ever be smaller than 1 Mev, it is seen that almost always $\exp[2(a_nR_n)^{\frac{1}{2}}]\gg1$ and $\exp[2(a_jR_j)^{\frac{1}{2}}]\gg1$. Equations (10) and (13) can thus be simplified, without introducing an appreciable error, to have the following forms:

$$\Gamma_n\simeq\frac{m_n r_0^2}{2\pi\hbar^2}\exp\{-2[a_0(E-\delta_0)]^{\frac{1}{2}}\}A_n^{\frac{2}{3}}\frac{g_n\alpha}{a_n^2}\exp[2(a_nR_n)^{\frac{1}{2}}]$$
$$\times\{2a_nR_n-(\tfrac{3}{2}-a_n\beta)[2(a_nR_n)^{\frac{1}{2}}-1]\},\quad(15)$$

and for charged particles

$$\Gamma_j\simeq\frac{m_j r_0^2}{2\pi\hbar^2}\exp\{-2[a_0(E-\delta_0)]^{\frac{1}{2}}\}A_j^{\frac{2}{3}}\frac{g_j(1+c_j)}{a_j^2}$$
$$\times\exp[2(a_jR_j)^{\frac{1}{2}}]\{2a_jR_j-\tfrac{3}{2}[2(2_jR_j)^{\frac{1}{2}}-1]\}.\quad(16)$$

Finally the two sides of Eqs. (15) and (16) were multiplied by $\exp\{-2[(a_jR_j)_{\max}]^{\frac{1}{2}}\}$, where $(a_jR_j)_{\max}$ is the largest value of aR among all possible reactions (including neutrons and charged particles). This procedure eliminates positive exponentials (which cannot be computed directly by the computer) and, on the other hand, avoids the use of excessive scaling factors which would impair the accuracy of the calculation.

(d) Kinetic Energy Selection

The kinetic energy distribution of outgoing neutrons is given by Eq. (7) and that of charged particles by the analogous equation with the subscript j instead of n, with α replaced by $(1+c_j)$, and $-\beta$ replaced by k_jV_j. In the Mark II program[1] the kinetic energies of the outgoing neutrons were assumed to have a Maxwellian distribution. A particular value of the kinetic energy was chosen from a table of the cumulative Maxwell distribution by means of a random number. For a charged particle the effective Coulomb barrier energy k_jV_j was added to the value so chosen to give the total kinetic energy of the charged particle. This approximation is valid if the excitation energy of the residual nucleus is large compared to the kinetic energy of the outgoing particle. For the calculations discussed in this paper this approximation is in general not valid. Hence it was decided to use the more accurate Eq. (7) for the kinetic energy distribution. To simplify the notation, the substitution $X=\epsilon-V$ was made, where $V=k_jV_j$ for charged particles and $V=-\beta$ for neutrons. By differentiation the value $X_{\max}$ for which $P(X)$ is a maximum may be found to be

$$X_{\max}=a_j^{-1}[(a_jR_j+1/4)^{\frac{1}{2}}-1/2],$$

and now $P(X)$ may be normalized to $P(X_{\max})=1$; it then becomes

$$P(X)=\frac{X}{X_{\max}}\exp\{a_jX_{\max}-[a_j(R_j-X)]^{\frac{1}{2}}\}.\quad(17)$$

The actual choice of a particular value of X involves the consecutive drawing of two random numbers between 0 and 1. The first random number, ξ_1, is used to choose a value of X between 0 and R_j—the maximum possible kinetic energy for the given particle j:

$$X=\xi_1R_j.$$

The second random number ξ_2 determines whether this value of X is to be accepted [if $P(X)>\xi_2$] or rejected [if $P(X)\leqslant\xi_2$].

If the particle to be emitted is a neutron, $X-\beta$ is checked before ξ_2 is chosen and if it is found negative, the particular value of X is rejected and a new random number ξ_1 chosen. This procedure is necessary since $X-\beta<0$ would correspond to a neutron of negative kinetic energy. As an illustration, the spectrum of neutrons emitted by Ge^{68} at 20-Mev excitation as calculated according to Eq. (17) is shown in Fig. 3.

The "negative barrier" ($V=-\beta$) in this case is 0.059 Mev.

It is seen from the shape of the spectrum in Fig. 3 that, for $X>X_{\max}$, $P(X)$ rapidly decreases and hence the probability of "success" in the kinetic energy selection $[P(X)>\xi_2]$ decreases rapidly. In order to save computer time, the field of search was limited in the following way. The range of possible kinetic energies of the outgoing particle was divided into three regions, and a different procedure was used for each. (a) For the region $X\leqslant 2X_{\max}$ the normalized $P(X)$ was computed from Eq. (17) and the value compared with ξ_2. If the computed value was smaller than ξ_2, it was rejected and a new random number ξ_1 chosen. If the computed value of $P(X)$ was greater than ξ_2, the kinetic energy chosen by the first random number ξ_1 was accepted and its value computed: $\epsilon=X+V$.[33] (b) In the second region, $2X_{\max}<X<11X_{\max}$, use was made of the fact that, for any positive value of X, the probability given by a Maxwell distribution:

$$P_M(X)=\frac{X}{X_{\max}}\exp[1-(X/X_{\max})], \qquad (18)$$

is greater than (or, for $X=X_{\max}$, equal to) that given by Eq. (17). A short table of values of $P_M(X)$ was stored in the memory of the computer and ξ_2 checked against the value of $P_M(X)$ interpolated from this table for the given value of X. If the random number was smaller than $P_M(X)$ the probability $P(X)$ was computed and the procedure described in (a) followed. In Fig. 3, $P_M(X)$ is shown for comparison with the spectrum obtained from Eq. (17). The spectra given by Eq. (18) are essentially those used in the Mark II program (except for a normalization factor). (c) A value of X in the third region, $X\geqslant 11X_{\max}$, was rejected without further calculation as fewer than 10^{-4} of the particles are emitted in this energy range.

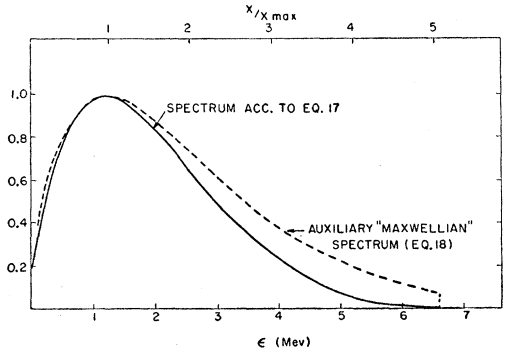

FIG. 3. Energy spectrum of neutrons emitted from Ge^{68} at 20-Mev excitation, according to Eq. (17). The auxiliary Maxwellian spectrum [Eq. (18)] is also shown. The ordinate scale is normalized to $P(X_{\max})=1$. Abscissa scales are given both in terms of the neutron energy in Mev, and of the ratio $X/X_{\max}$.

[33] The residual excitation energy E_j remaining after particle j is evaporated with kinetic energy ϵ_j was taken as $E_j=E-Q_j-\epsilon_j-V=R_j-\epsilon_j+\delta_j$.

(e) Q Values

Wherever possible, Q values based on experimental data were used in Eqs. (11) and (14). They were computed from the atomic mass data compiled by Wapstra,[34] supplemented by more recent data on Cr^{48},[35] Fe^{52},[35] Ni^{56},[35] Zn^{61},[36] Zn^{71},[35] Zn^{72},[35] Ge^{65},[37] Ge^{68},[35] As^{69},[35] As^{70},[35] Se^{70},[35] and Se^{72}.[38] For nuclei for which experimental mass values were not available, the masses computed by Cameron[39] from his semiempirical mass formula were used. The mass data were stored in the computer memory in the form of a table listing the mass excess $(M-A)$.

(f) Computation Procedure

The input data for each computation included A, Z, and excitation energy of the starting nucleus, the number of cascades to be followed, and various parameters such as the value of A/a. Tables of δ values were also stored in the memory.

For each initial condition, the relative emission probabilities for neutrons, protons, deuterons, tritons, He^3, and He^4 particles were computed according to Eqs. (15) and (16). From the cumulative sum of these probabilities normalized to 1, the emitted particle was selected by means of a random number between 0 and 1. The kinetic energy of this particle was then selected according to the procedure outlined in Sec. IId. A, Z, and excitation energy of the residual nucleus were computed and the procedure was repeated with this as a starting point. The evaporation cascade was terminated when none of the R values [see Eqs. (11) and (14)] was greater than 0, whereupon a new cascade was started with the original A, Z, E values. The procedure used involves the assumption that gamma de-excitation takes place whenever particle emission is energetically prohibited, but does not compete with particle emission above this limit.

After the specified number of cascades—usually 500—had been calculated, the computer summarized the results. The output data included the following information: the total number of each type of particle emitted; either the energy spectra of the evaporated particles or the spectra of residual excitation energies at various stages of the cascade; the number of cascades resulting in each final product nuclide; the details of the evaporation path in the form of the number of each intermediate and final product arising through the emission of each type of particle. To gain some insight into the magnitude of the statistical fluctuations in the calculated yields of the various reaction products, the

[34] A. M. Wapstra, Physica **21**, 385 (1955).
[35] Strominger, Hollander, and Seaborg, Revs. Modern Phys. **30**, 585 (1958).
[36] J. B. Cumming, Phys. Rev. **114**, 1600 (1959).
[37] N. T. Porile, Phys. Rev. **112**, 1954 (1958).
[38] J. B. Cumming and N. R. Johnson, Phys. Rev. **110**, 1104 (1958).
[39] A. G. W. Cameron, Atomic Energy of Canada Limited Report CRP-690, 1957 (unpublished).

TABLE III. Fluctuation of the calculated yields of various products from Ni^{58} and Fe^{58} compound nuclei at 25-Mev initial excitation.

Compound nucleus	Emitted particles	Number of reactions of specified type recorded in each group of 500 cascades										Mean	Standard deviation
Fe^{58}	n	50	76	65	61	64	65	79	73	75	69	67.7	± 8
	$2n$	442	410	425	428	419	424	411	416	416	418	421	± 9
	p	4	4	6	7	5	3	7	4	6	7	5.3	± 2.3
	α	4	10	4	4	12	7	3	7	3	6	6.0	± 2.9
Ni^{58}	p	312	326	326	335	305	331	312	307	333	325	321	±11
	n	119	100	114	106	123	103	119	127	112	115	114	± 8
	pn	49	54	48	49	55	51	52	55	45	54	51	± 3
	$2p$	9	9	7	6	8	8	10	6	6	2	7.1	± 2.2
	α	11	11	5	4	9	7	7	5	4	4	6.7	± 2.5

computation for the two compound nuclei Ni^{58} and Fe^{58} at 25 Mev excitation was repeated 10 times (with 500 cascades each), with all parameters unchanged but with a different initial random number each time. The results are shown in Table III. It is seen that for the minor products the fluctuation is, to a good approximation, Poissonian. For the higher-yield products the fluctuation is much smaller than $\pm\sqrt{n}$. As an illustration, the statistical errors have been indicated in the plots of the calculated excitation functions of the reactions of the Ga^{67} compound nucleus (Fig. 19).

III. COMPARISON WITH EXPERIMENTAL DATA

(a) Effects of Various Assumptions and Parameters

To examine, as a first step, the influence of the various refinements introduced into the computations (Sec. II above) a few cross-section ratios were computed with both the old (Mark II) and new (Mark IIc) programs. The nuclei chosen are listed in Table IV together with the excitation energies at which the comparisons were made; the latter were taken near the peaks of the excitation functions of the respective products. To separate the effect of introducing pairing and shell corrections in the level density expression from that of the other changes made, both programs were used with and without Cameron's δ values[17] and a 1-Mev shell correction. The computed cross-section ratios are presented in Table IV. 500 evaporation cascades were computed for each nuclide. Inspection of columns 5 and 6 shows that the neutron emission probability tends to be higher relative to charged-particle emission with the new program than with the old. This is presumably caused by the fact that the inverse reaction cross section for neutrons has been increased more than that for charged particles. The change from the Mark II to the Mark IIc program alone made altogether surprisingly little difference in the ratios listed, perhaps as a result of compensating effects.

TABLE IV. Comparison of cross-section ratios computed with various sets of assumptions.

Compound nucleus	Excitation energy (Mev)	Emission ratio	Experimental value	Computed values: Mark II No δ's	Mark IIc No δ's	Mark II Cameron δ's	Mark IIc Cameron δ's
Se^{74}	35	$pn/2n$	1.7	0.29	0.25	1.22	1.0
Ge^{68}	20	p/n	1.76	1.43	1.07	1.57	0.95
	35	$pn/2n$	8.4	0.84	0.76	8.3	7.8
	40	$2pn/p2n$	5.8	0.73	0.61	0.58	0.35
	40	$\alpha pn/\alpha 2n$	4.1	0.07	0.06	4.0	4.1
Ga^{67}	35	$pn/2n$	3.3	2.3	2.1	2.0	1.3
Ni^{58}	25	p/n	3.8	0.67	0.79	2.9	2.5
	35	$pn/2n$	67	0.73	0.51	6.2	59
	40	$2pn/p2n$	7.3	2.8	0.61	3.3	5.3
Fe^{54}	35	$pn/2n$	31	0.56	0.69	7.2	8.3
Mn^{54}	30	$pn/2n$	<1	8.9	7.8	0.59	0.52
Cr^{50}	25	p/n	0.51	0.73	0.85	0.90	0.78
	35	$pn/2n$	46	0.52	0.55	6.4	5.4

The most striking effect seen in Table IV is that, in general, the agreement with experiment is greatly improved with the introduction of the pairing and shell corrections. However, even with the δ's taken from Cameron[17] the agreement is in many cases still unsatisfactory. It seemed of interest, therefore, to explore whether changes in the values of the δ's would lead to improved agreement with experiments. In other words, for the present, the δ values were considered as adjustable parameters, without an attempt to justify their values in detail in terms of a physical picture.

The degree of agreement between calculated and experimental excitation functions depends not only on the set of δ values used, but also on the magnitude of a. To examine the effects separately, computations were carried out with a given set of δ's, but with varying values of a. As shown in Table V, the relative cross sections of reactions involving the emission of equal numbers of nucleons are, at least near the excitation function peaks, not strongly affected by the choice of a, whereas it is just these ratios which are sensitive to the δ values. The value of a, on the other hand, does affect the shapes of the excitation functions as shown in Fig. 4. The δ choices turned out to have rather little effect on these shapes although large changes in δ's cause shifts in excitation curves as might be expected. It was thus in first approximation possible to separate the

effects of a and δ and to adjust their values more or less independently as already noted by Porile.[11]

In Fig. 4 are plotted the calculated excitation curves for the $(\alpha,n)+(\alpha,p)$, $(\alpha,2n)+(\alpha,pn)$, and $(\alpha,3n)+(\alpha,p2n)+(\alpha,2pn)$ reactions of Zn^{64}, for $a=A/10$, $A/20$, and $A/40$, together with the experimental curves.[11] It is seen that, with increasing a, the slopes on both wings of an excitation function become steeper. This effect is a direct consequence of the change with a of the spectra of emitted particles. As a increases, the nuclear temperature at a given excitation energy decreases and therefore the spectrum of emitted particles is expected to shift to lower energies. This effect is illustrated in Fig. 5. A shift in particle spectra to lower energies is equivalent to a shift in residual excitation energy spectra to higher energies and therefore leads to an increased probability for the emission of an additional particle. Thus the drop as well as the rise of cross sections with increasing energy is expected to be steeper with large than with small a, and this prediction is borne out by the detailed calculations. The calculations to be discussed in the remainder of this paper were carried out with $a=A/20$ which gave in most cases a somewhat better fit to the experimental data than either $a=A/10$ or $a=A/40$.

TABLE V. Comparison of cross-section ratios computed with Cameron's δ set, but with different values of a.

Target nucleus	Compound nucleus	Excitation energy (Mev)	Reaction ratio	Computed ratio for $a=A/10$	$a=A/20$	$a=A/40$	Experimental ratio
Zn^{64}	Ge^{68}	35	$(\alpha,pn)/(\alpha,2n)$	8.0	7.8	6.0	8.4
Zn^{64}	Ge^{68}	20	$(\alpha,p)/(\alpha,n)$	0.97	0.95	0.99	1.8
Cu^{65}	Ga^{69}	30	$(\alpha,pn)/(\alpha,2n)$	···	0.50	0.51	···
Ti^{46}	Cr^{50}	45	$(\alpha,p2n)/(\alpha,2pn)$	2.0	1.7	···	···
Ti^{46}	Cr^{50}	30	$(\alpha,n)/(\alpha,p)$	1.4	1.3	···	2.0

(b) Criteria for Adjustment of δ Values

Before proceeding with the exploration for a set of δ's which would lead to better agreement with experiment it was necessary to consider the nuclei, reactions, and energies most suitable for this purpose. In order to minimize the dependence on a and the effects of threshold shifts inherent in the formalism (see Sec. IIc), attention was focussed on reactions near the peaks of their excitation curves. For a variety of other reasons, not all the reactions listed in Table I were considered suitable as a basis for the initial δ adjustments. Fitting was not attempted in the region of high-energy tails of excitation functions [such as (α,n) and (α,p) reactions at 40 Mev] because of the likelihood of reaction mechanisms other than compound nucleus formation. Alpha-induced reactions involving re-emission of alpha particles were eliminated from the fitting procedure because there is independent evidence[40] from alpha-particle spectra and angular distributions that such reactions proceed, at least partially, through direct-interaction mechanisms. For the same reason, (p,pn) reactions were not used. Reaction cross sections of less than a few millibarns [such as the $Zn^{70}(\alpha,2p)$ reaction[12]] were, of course, not useful for quantitative comparisons because of the limited statistics of the calculations. The data of Meadows[9] and Ghoshal[8] on reactions involving the compound nucleus Zn^{64} are discrepant with respect to cross section and energy scale and were therefore not used. The $V^{50}(\alpha,2p)$ and $V^{50}(\alpha,2n)$ data of Chasman and Friedlander[3] were not considered sufficiently accurate to be included in the fitting procedure.

On the basis of the above considerations, the compound nuclei, excitation energies, and cross-section

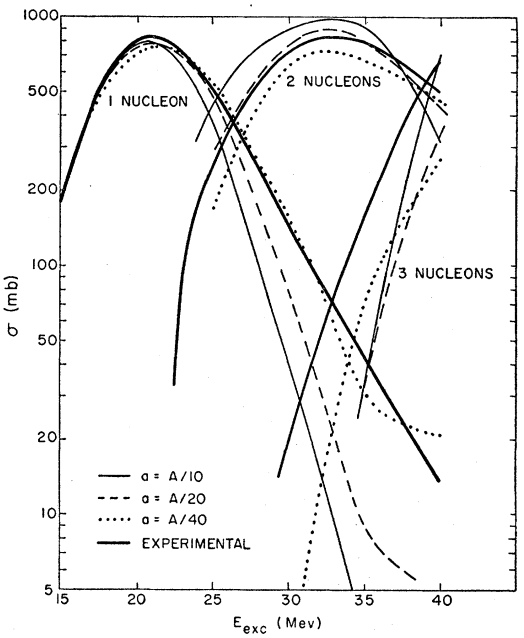

FIG. 4. Comparison of calculated and experimental[11] excitation functions for one-, two-, and three-nucleon emission reactions produced in the interaction of Zn^{64} and α particles.

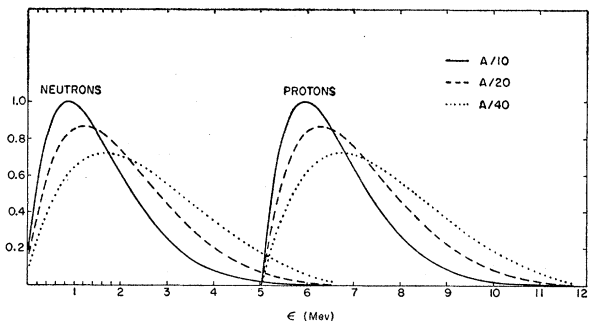

FIG. 5. Energy spectra of neutrons and protons emitted from Ge^{68} at 20-Mev excitation, calculated with different values of a. The ordinate scale is normalized to $P(X_{max})=1$ for $a=A/10$, and the curves for different a values are normalized to the same total area.

[40] G. Igo, Phys. Rev. **106**, 256 (1957).

TABLE VI. Nuclei and reactions selected to check goodness of fit for various sets of δ's.

Compound nucleus	Excitation energies (Mev)	Particle emission ratios	δ's involved Z	N
Cr^{50}	45	$(3n+p2n)/3p$	22, 24	24, 26
	40–45	$2n/pn$	24	24, 26
	25	n/p	24	26
Fe^{54}	25–45	$2n/pn$	26	26, 28
Ni^{58}	45	$p2n/2pn$	26, 28	28, 30
	30–40	$2n/pn$	28	28, 30
	20–25	n/p	28	30
Ga^{67}	30–40	$2n/pn$	30	34, 36
Ga^{69}	35–40	$2n/pn$	30	36, 38
Ge^{68}	40	$3n/p2n/2pn$	30, 32	34, 36
	30–35	$2n/pn$	32	36
	20–25	n/p	32	36
Se^{74}	30–40	$2n/pn$	34	38, 40

ratios listed in Table VI were used for the initial δ-fitting. As will be seen from the table, all δ's from $Z=22$ to $Z=34$ and from $N=24$ to $N=40$ with the exception of δ for $N=32$ can be determined from this set of reactions. In fact most of the δ's are overdetermined. As an aid in the determination of the goodness of fit of a particular set of calculations, the computed and experimental results were compared as follows. For each compound nucleus and each energy, the yield of each reaction of interest was computed as a fraction of the sum of all the reaction yields of interest, and the difference between this calculated fractional yield and the corresponding experimental fractional yield was squared. The sum of the squares for all the reactions considered was taken as a measure of the goodness of fit. In using this criterion, the statistical fluctuations in the computed yields and the experimental uncertainties had to be taken into account.

After a "good" set of δ's had been chosen on the basis of these criteria and with the aid of the procedures outlined in the following section, it proved profitable to make some final adjustments on the basis of complete excitation functions, i.e., taking into account not only cross-section ratios, but also absolute values and energy dependence.

(c) Adjustment of δ Values

For the first step in adjusting δ values it is convenient to consider the competition between reactions involving the emission of one nucleon, at an energy where no other reactions are significant. In this situation the ratio Γ_n/Γ_p directly determines the relative cross sections for neutron and proton emission. For an even-mass compound nucleus neutron emission and proton emission probabilities are each affected by one δ value only. Thus, if the ratio of neutron and proton emission cross sections is available from experimental data, one can determine a locus of pairs of these values which give the correct Γ_n/Γ_p ratios at a given initial excitation energy. The loci proved to be nearly straight lines as shown in Fig. 6. As may be seen, the positions of the lines depend somewhat on the excitation energies; but this dependence is least in the region of the peaks of the one-particle excitation functions, and the data in this region were used.

The use of the loci just discussed reduces the number of adjustable parameters. In the subsequent fitting procedures, the proper relation between the pairs of δ values for which loci were available was always maintained. For reactions involving the emission of two or more particles no simple procedures for adjustment of δ's were available. However, by examining the evaporation paths in detail, one can fairly easily determine which δ's need to be adjusted, and in what direction, for the rectification of major discrepancies. The procedure is illustrated for the Ga^{67} compound nucleus at 35-Mev excitation in Figs. 7 and 8. In Fig. 7 the evaporation path obtained with Cameron's δ set is shown; the number of events proceeding along each

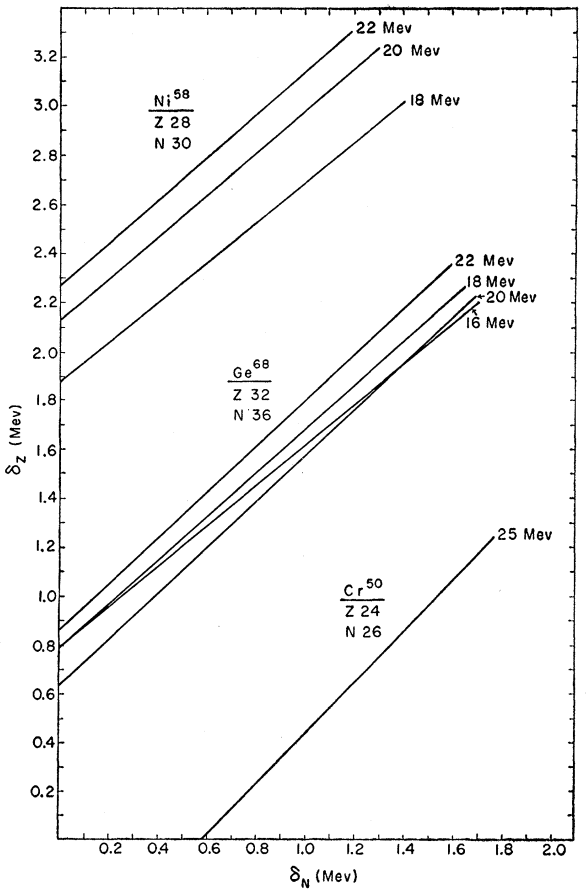

FIG. 6. Loci of δ_N and δ_Z values for the products of proton and neutron emission from the compound nuclei Cr^{50}, Ni^{58}, and Ge^{68}, obtained from the measured proton-neutron emssion ratios at several excitation energies.

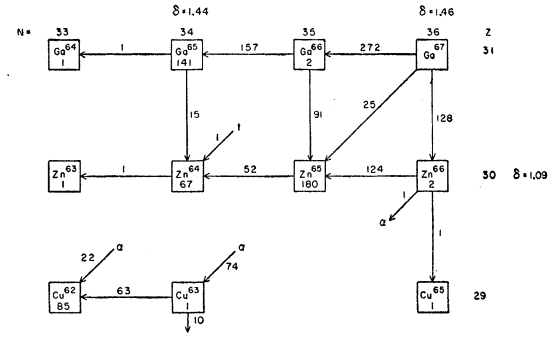

FIG. 7. Computed evaporation paths for 500 Ga^{67} nuclei at 35-Mev initial excitation. Cameron's δ values were used. The computed numbers of evaporated particles are given alongside the corresponding arrows. The numbers in the boxes indicate the numbers of product nuclei formed. The δ values are given in Mev. *Note.* The number 180 should read 188.

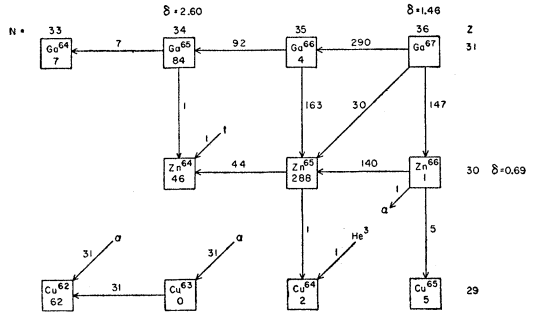

FIG. 8. Evaporation paths for 500 Ga^{67} nuclei at 35-Mev excitation, computed with δ values modified as shown (in Mev). See Fig. 7 for comparison.

path, out of a total of 500 events, is indicated. The number of evaporation cascades ending at each nuclide is shown also. The numbers of residual Ga^{65} and Zn^{65} nuclei are seen to be 141 and 188, respectively, whereas the experimental results,[10] in the same units, are 105 and 320. In order to decrease the computed yield of Ga^{65} and increase that of Zn^{65}, it was decided to raise δ_{N34} and lower δ_{Z30}. The flow diagram obtained with this new δ set (with $\delta_{Z30}=0.69$ Mev, $\delta_{N34}=2.60$ Mev) is shown in Fig. 8. The Ga^{65} and Zn^{65} yields are now seen to be 84 and 288 nuclei, respectively. Thus too much of a decrease in the calculated Ga^{65} yield has been accomplished, whereas Zn^{65} formation has not been increased quite enough; but the new results are much closer to the experimental values than the previous ones. With further changes in δ's the agreement can be further improved. It may be noted that the increase in Zn^{65} yield was achieved by an increased feed-in (due to the lowering of δ_{Z30}) as well as a decreased outflow (due to the over-all increase in the δ of Zn^{64}). Another interesting effect is seen in Ga^{65}, where the increase in δ_{N34} decreases *both* the inflow from Ga^{66} and the outflow to Zn^{64}. In the present situation, the first effect predominates, leading to a net decrease in Ga^{65} yield. As mentioned below, the opposite net effect may also occur in some circumstances. Finally it may be noted that the α-particle emission from Ga^{67} has been greatly reduced by the increase in δ_{N34} (directly affecting Cu^{63}); on the other hand, α emission from Ga^{66} has been increased, not because the product Cu^{62} involves a δ, but because this α emission can compete more effectively when the neutron emission to Ga^{65} is hindered by a high δ_{N34}.

Whereas it is relatively simple to obtain a good fit to experimental data for a given pair of cross-section ratios in the manner just illustrated, the over-all problem is much more complex. In the first place, any given δ value is generally involved in more than one reaction for which experimental data are available and the requirements for fitting different cross-section ratios are sometimes difficult to reconcile. In the second place, a change in δ has subtler effects in addition to the ones illustrated, and these come into play when fine adjustments are attempted. Thus a change in δ's affects the excitation energy distribution of the residual nuclei. In particular, an increase in the δ for the product of a given evaporation step will increase the average excitation energy of this residual nucleus. This is caused by the fact that the increase in the δ reduces the maximum possible kinetic energy of the emitted particle ($R=E-Q-V-\delta$).

Another effect, albeit an artificial one (see Sec. II), which occurs in 2- or 3-particle emission reactions, is the change (by an amount equal to the δ of the final product) of the energy cutoff point in the excitation energy spectrum of an intermediate nucleus, below which no evaporation is possible. This effect leads to a shift to higher energies (by δ) of the threshold for the particular reaction involving the δ and thus to some distortion of the excitation function.

Another complicating feature is that the effect of a change in δ on the yield of a particular nuclide involving that δ value is energy dependent and may even reverse direction. When the product of interest is formed at sufficiently low excitation to be the terminal product, an increase in its δ value will inhibit its formation (see

TABLE VII. δ values.

Z or N	δ_Z in Mev		δ_N in Mev	
	Cameron[a]	Present work (DFF)	Cameron[a]	Present work (DFF)
22	1.73	1.18		
24	1.44	1.38	1.41	1.90
26	1.45	0.87	1.29	1.90
28[b]	1.37	2.76	1.47	2.47
30	1.07	0.50	1.32	0.50
32	1.36	1.35	1.46	2.06
34	1.42	1.82	1.44	1.90
36			1.46	0.50
38			1.52	2.00
40			1.51	1.41
42			1.47	1.70

[a] See reference 17.
[b] No shell effects are included in Cameron's values, whereas they are in the DFF values.

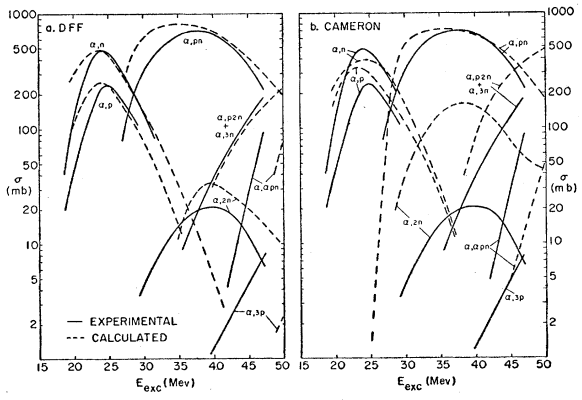

FIG. 9. Experimental[2] and calculated excitation functions for reactions of Ti^{46} with α particles (compound nucleus Cr^{50}).

the example of Ga^{65} in Figs. 7 and 8). At higher excitations, where further evaporation is possible, the same δ value affecting the nuclide under discussion will also control the formation of one of the further evaporation products and may have a greater effect on the disappearance of the nuclide than on its formation.

(d) Symmetry Effect

In attempting to obtain good agreement with experimental cross sections of the $Cr^{50}(\alpha,2n)^4$ and $Ti^{46}(\alpha,2n)^2$ reactions, which are unusually low, it was found necessary to add another term to the δ's of $_{24}Cr^{48}$ and $_{26}Fe^{52}$. The calculated production rates of these two nuclei could not be made sufficiently small by adjustments of the δ values for $N=24$, 26 and $Z=24$, 26, without destroying the agreement for other nuclides with these neutron and proton numbers. A specific, additional δ of 2 Mev was found necessary for these nuclei with $Z=N$. This empirical result which appears to indicate a particular scarcity of available levels in such symmetric nuclei has been interpreted by de-Shalit[41] in terms of the particular purity of states of isotopic spin $(T)=0$; the transition probabilities from the compound states to these very pure $T=0$ states are very small and thus the levels to which neutron or proton evaporation can take place should, in first approximation, be counted from the lowest lying state of $T\neq 0$. From the energies of the ground states of neighboring isobars, the lowest

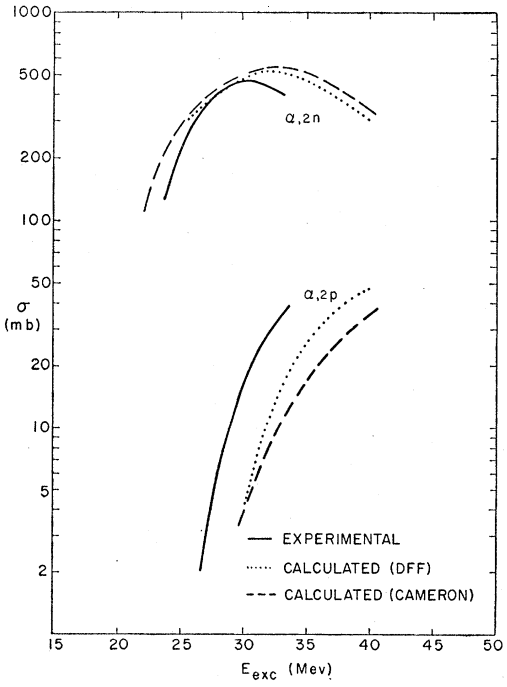

FIG. 10. Experimental[3] and calculated excitation functions for reactions of V^{50} with α particles (compound nucleus Mn^{54}).

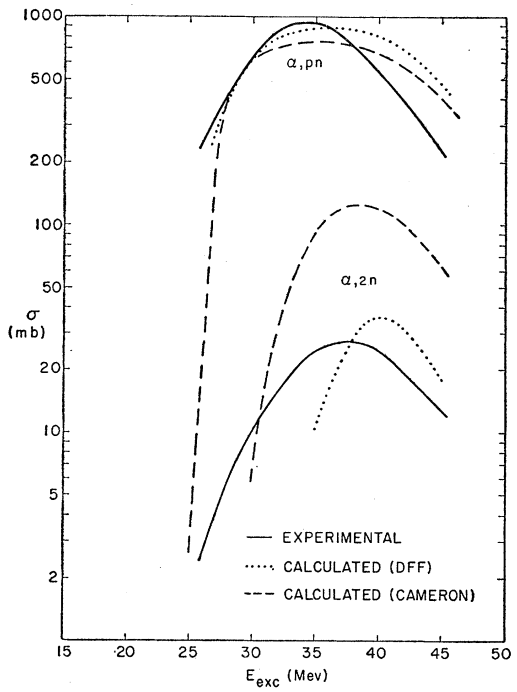

FIG. 11. Experimental[4] and calculated excitation functions for reactions of Cr^{50} with α particles (compound nucleus Fe^{54}).

lying states of $T=1$ in Cr^{48} and Fe^{52} are estimated to be of the order of 2 Mev above the ground states, in agreement with the characteristic-level displacement arrived at empirically.

The other symmetrical nucleus which has been investigated in this region, $_{28}Ni^{56}$, is formed in extremely low cross section also[6]; but it was found that the δ values for $Z=28$ and $N=28$ (which include shell effects) were sufficiently large to suppress the computed formation cross section of the doubly magic Ni^{56} to almost the required extent (see Fig. 12). The inclusion of a 2-Mev symmetry correction inhibited the formation of Ni^{56} to too large an extent. On the basis of de-Shalit's

[41] A. de-Shalit (private communication).

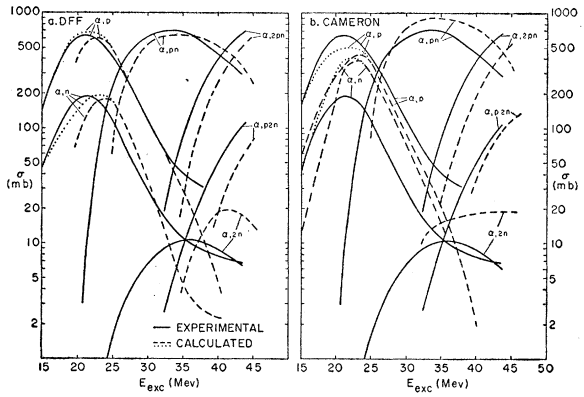

FIG. 12. Experimental[6] and calculated excitation functions for reactions of Fe^{54} with α particles (compound nucleus Ni^{58}). At low energies, the dashed curves were normalized to the continuum theory cross sections, the dotted curves to the sum of the experimental values.

explanation[41] a symmetry correction should not be needed for a doubly magic nucleus, as may again be deduced by reference to the ground-state positions of neighboring isobars.

It should be pointed out that the symmetry correction under discussion here has nothing to do with the very small isotopic-number dependence of the level density parameter introduced by Le Couteur.[29] The effect of the latter on the computed formation cross sections of symmetric nuclei is negligible, and the physical bases of the two effects are quite different.

(e) Comparison of Calculated and Measured Excitation Functions

Using the procedure described and the considerations just mentioned, δ values were successively varied until

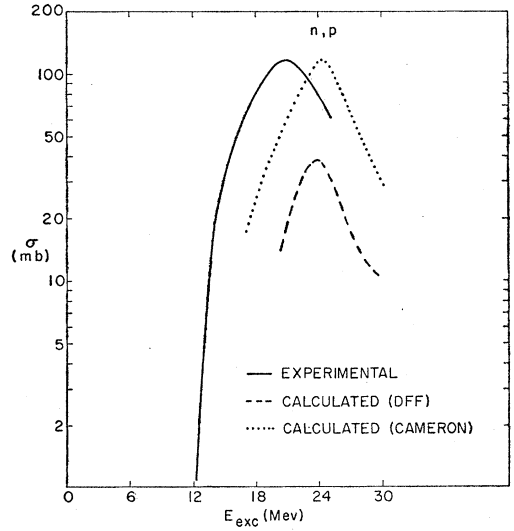

FIG. 13. Comparison of calculated $Fe^{56}(n,p)Mn^{56}$ excitation functions with the experimental data of Terrell and Helm.[5]

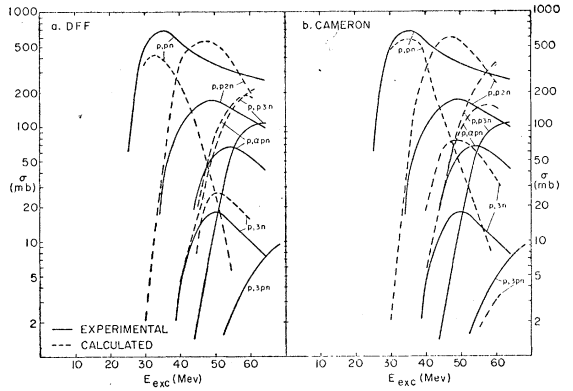

FIG. 14. Experimental[7] and calculated excitation functions for reactions of Co^{59} with protons (compound nucleus Ni^{60}).

a set was arrived at, which gave a reasonably good fit to the data of Table VI. This set, henceforth referred to as the DFF set of δ values, is shown in Table VII, together with the values given by Cameron. It should by no means be concluded that this represents "the best possible set" of δ values out of the entire matrix of possible combinations. To explore this matrix completely would have taken an undue amount of labor and computer time. In any case, anyone now setting out to explore whether a unique and consistent set of δ values exists and to determine such a set could, with proper design of experiments, do so without recourse to Monte Carlo calculations as will be discussed in Sec. VI.

With the DFF set of δ values and the symmetry correction discussed above, excitation functions were computed for all reactions listed in Table I. It should be noted that this is a much more extensive list than that used for the actual fitting of the δ values (Table VI). These excitation functions, together with the experimentally determined ones, are shown in Figs. 9–24. For comparison, the excitation functions computed with Cameron's δ set are also shown. It is seen that, for almost all nuclei, the agreement of the experimental results with those calculated using the DFF set

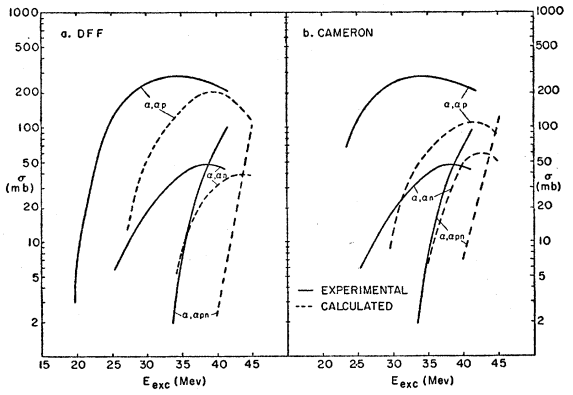

FIG. 15. Experimental[6] and calculated excitation functions for reactions of Ni^{58} with α particles (compound nucleus Zn^{62}).

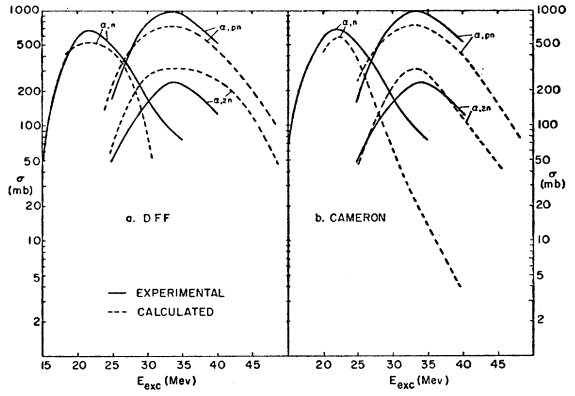

FIG. 16. Experimental[8] and calculated excitation functions for reactions of Ni^{60} with α particles (compound nucleus Zn^{64}).

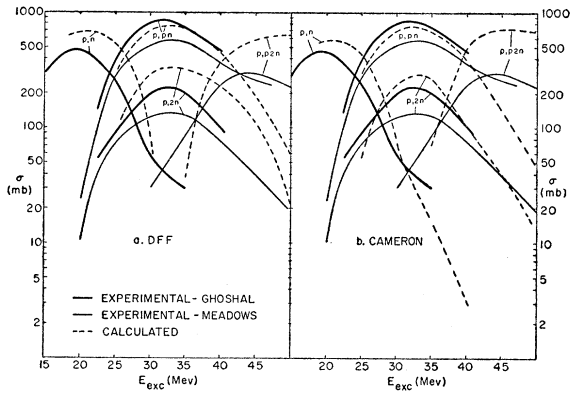

FIG. 17. Experimental[8,9] and calculated excitation functions for reactions of Cu^{63} with protons (compound nucleus Zn^{64}).

of δ's, while not entirely satisfactory, is better than with those computed using Cameron's δ's.

In addition to the excitation functions shown, a few cross sections known at single energies were calculated. The results are shown in Table VIII, together with the experimental data. The agreement is seen to be rather satisfactory except in the case of the ratio of $(p,pn)/(p,2n)$ cross sections of Ga^{69}; the fact that this ratio is underestimated by the calculations probably stems from the low value of δ_{N36} in the DFF set; this is discussed below. It is interesting to note that, for Ni^{58}, the computations yield a very high $(p,2p)$ cross section, in agreement with the experimental result of Cohen *et al.*,[42] but entirely on the basis of a compound nucleus mechanism rather than through direct interaction as postulated by Cohen.[43] This result does, of course, not prove that the reaction proceeds predominantly through a compound nucleus, but it may throw some doubt on Cohen's conclusions.

In comparing the results of the computations with experimental data one must, of course, make an assumption about the total capture cross sections for the bombarding particles used in the experiments. For consistency with the choice of $r_0=1.5\times10^{-13}$ cm in the Monte Carlo calculations, the continuum-theory cross sections[26] for this value of r_0 were used. For some reactions (e.g., $Zn^{64}+\alpha$, $Fe^{54}+\alpha$, $Cu^{65}+\alpha$) the sum of the experimentally determined cross sections at low energies actually exceeds the continuum-theory cross sections so computed; in these cases, the calculated excitation functions are shown with two alternative normalizations, i.e., to the continuum-theory cross section and to the sum of experimental cross sections. An error in the energy dependence of total cross sections arising from inadequacies of the continuum theory or from unsuitable choice of r_0 gives rise to some distortion of the computed excitation curves, particularly at low energies. It should also be kept in mind that the absolute values of most experimental cross sections have uncertainties of the order of $\pm10\%$ (although some cross-section *ratios* are quoted to $\pm5\%$) and that the energy scales of the experimental curves may be distorted, especially at low energies, because of energy straggling in beams of degraded particles and uncertainties in range-energy relations. These difficulties are

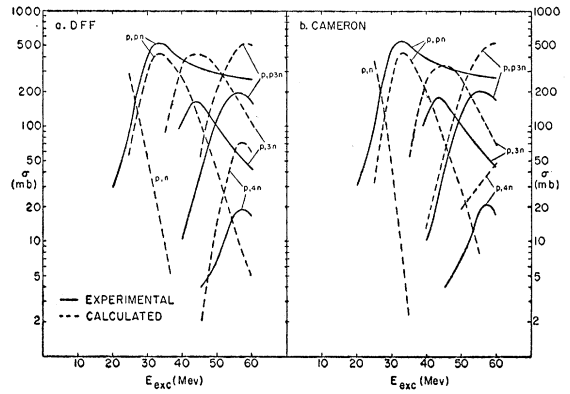

FIG. 18. Experimental[9] and calculated excitation functions for reactions of Cu^{65} with protons (compound nucleus Zn^{66}).

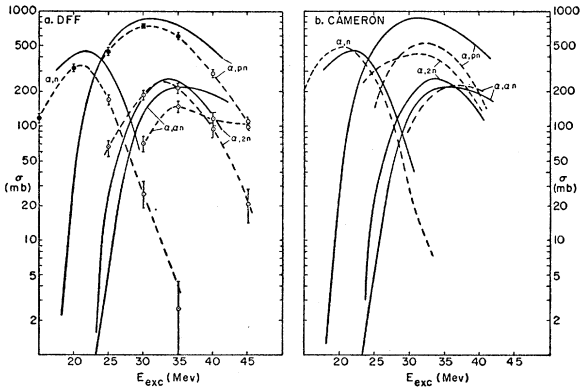

FIG. 19. Experimental[10] and calculated excitation functions for reactions of Cu^{63} with α particles (compound nucleus Ga^{67}). The approximate statistical uncertainties of the calculated points are indicated in graph a.

[42] Cohen, Newman, and Handley, Phys. Rev. **99**, 723 (1955).
[43] B. L. Cohen, Phys. Rev. **108**, 768 (1957).

illustrated in Fig. 17 where data by different authors for the Zn^{64} compound nucleus (from $Cu^{63}+p$) are shown.

As was discussed earlier, the introduction of δ values is equivalent to the assumption that, in all but the odd-odd nuclei, no levels below a characteristic level are available. This approximation is bound to shift the thresholds of reactions leading to such nuclei. This effect can readily be seen in the comparison of the calculated and experimental curves. Where the δ values are very large (as for example in Fe^{52}), the shift may persist far beyond the threshold for the production of the nuclide in question and lead to considerable distortion of the computed curve, with even the peak of the excitation function shifted to higher energies (see Fig. 11). These shifts are expected only when the final product has a nonzero δ value and not as a result of δ's at intermediate nuclei along the evaporation path. The shift of the calculated $Zn^{65}(\alpha,n)$, $(\alpha,2n)$, and $(\alpha,3n)$ excitation functions (Ga^{69} compound nucleus) to *lower* energies (Fig. 20) is probably a consequence of the low

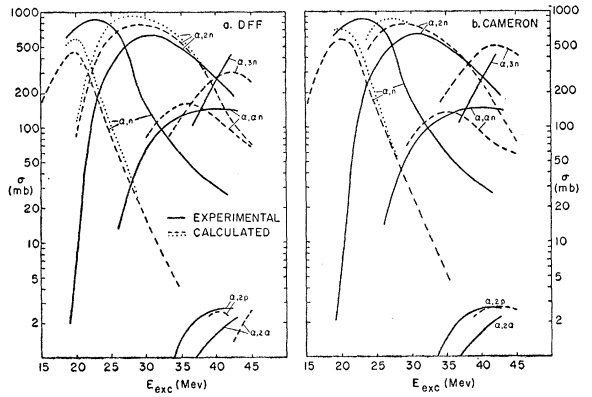

FIG. 20. Experimental[10] and calculated excitation functions for reactions of Cu^{65} with α particles (compound nucleus Ga^{69}).

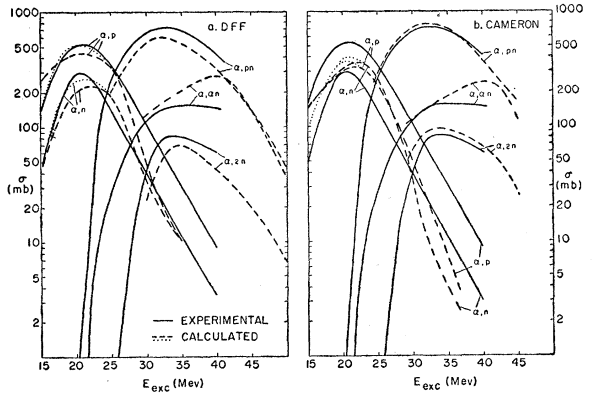

FIG. 21. Experimental[11] and calculated excitation functions for reactions of Zn^{64} with α particles (compound nucleus Ge^{68}) which lead to emission of one or two particles. At low energies, the dashed curves were normalized to the continuum-theory cross sections, the dotted curves to the sum of the experimental values.

TABLE VIII. Comparison of some calculated and experimental cross sections. (Calculations with the DFF δ set.)

Reaction	Compound nucleus	Incident energy in the laboratory system (Mev)	Excitation energy (Mev)	Cross section in mb: Experimental	Cross section in mb: Calculated	Reference
$Cr^{52}(p,2n)Mn^{51}$	Mn^{53}	21.5	29.7	155	167	a
$Cr^{52}(p,pn)Cr^{51}$				425	670	
$Fe^{56}(p,2n)Co^{55}$	Co^{57}	21.5	29.9	105	61	a
$Fe^{56}(p,pn)Fe^{55}$				760	850	
$Ni^{58}(p,2n)Cu^{57}$	Cu^{59}	21.5	32.7	240	3	b
$Ni^{58}(p,pn)Ni^{57}$					434	
$Ni^{58}(p,2p)Co^{57}$				680	840	
$Cu^{65}(n,2n)Cu^{64}$	Cu^{66}	14.1	21.0	970	1150	c
$Cu^{65}(n,p)Ni^{65}$				19	6	
$Ga^{69}(p,2n)Ge^{68}$	Ge^{70}	21.5	27.7	360	585	a
$Ga^{69}(p,pn)Ga^{68}$				360	120	

[a] B. L. Cohen and E. Newman, Phys. Rev. **99**, 718 (1955).
[b] From reference 42. The measured value of 240 mb is the sum of the $(p,2n)$ and (p,pn) cross sections.
[c] S. G. Forbes, Phys. Rev. **88**, 1309 (1952).

value of δ_{N36} and represents a certain inconsistency in the DFF δ set.

Examination of Figs. 9–24 shows that even with the DFF δ set some of the computed excitation functions exhibit sizable discrepancies from the experimental curves. Some of these discrepancies could almost certainly not be remedied by any other choices of δ values and are taken as evidence that mechanisms other than compound nucleus formation are operative in the reactions concerned. Perhaps the clearest examples are the (p,pn) reactions of Cu^{63} and Cu^{65} (Figs. 17 and 18) which do not drop off nearly as fast beyond the peaks of their excitation functions as the calculations predict. Thus at proton energies as low as 30 Mev (corresponding to computed excitations of the compound nucleus of approximately 38 Mev), these (p,pn) reactions appear to proceed to an appreciable extent by direct interaction. At higher energies (approximately 50-Mev proton energy) the rather large experimentally observed (p,pn) reaction cross sections must be caused almost entirely by direct interactions. As a consequence of the large direct interaction cross section for proton reactions at high energies, the compound nucleus formation cross sections are much smaller than the total reaction cross sections. A comparison of the experimental and calculated curves for $Cu^{65}+p$ (Fig. 18) leads to the conclusion that at 52-Mev proton energy (corresponding to 60-Mev excitation of the compound nucleus) only about 30% of the reactions proceed via compound nucleus formation. This is in good agreement with the predictions of the prompt-cascade calculations of Metropolis *et al.*[44] It should be noted that the *ratios* of more complex reactions ($3n$, $4n$, and $p3n$ emission) are well represented

[44] Metropolis, Bivins, Storm, Turkevich, Miller, and Friedlander, Phys. Rev. **110**, 185 (1958).

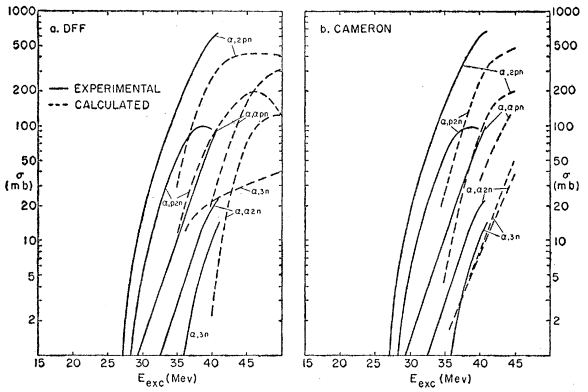

FIG. 22. Experimental[11] and calculated excitation functions for reactions of Zn^{64} with α particles (compound nucleus Ge^{68}) which lead to emission of 3 particles.

by the present calculations even at 60-Mev excitation energy. These reactions are thus unlikely to be produced to an appreciable extent by non-compound-nucleus mechanisms. The proton-induced reactions[7] of Co^{59} (Fig. 14) show very similar behavior.

The high-energy tails of (α,n) and (α,p) excitation functions such as are exhibited by the experimental data on $Fe^{54}+\alpha$ and $Cu^{65}+\alpha$ (Figs. 12 and 20) are not reproduced by the computations and are probably evidence for non-compound-nucleus mechanisms.

The α-particle-induced reactions involving re-emission of α particles were not used in the fitting procedure because it was thought likely that they proceed to a large extent by non-compound-nucleus mechanisms. However, examination of Figs. 15, 19, 21, and 22 shows that although the calculated excitation functions for

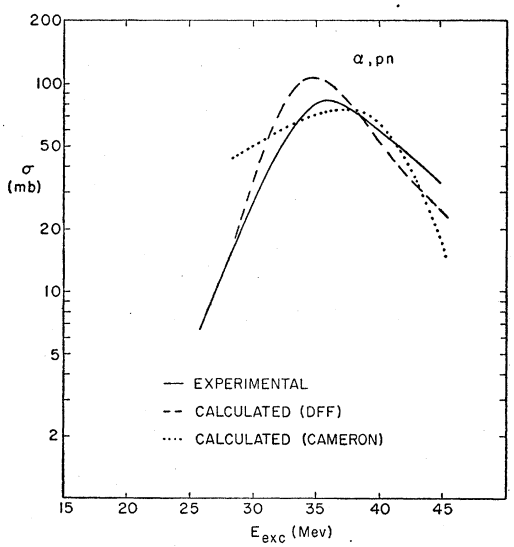

FIG. 23. Experimental[12] and calculated excitation functions for the $Zn^{70}(\alpha,pn)Ga^{72}$ reaction (compound nucleus Ge^{74}). The reaction $Zn^{70}(\alpha,2p)Zn^{72}$ was found[12] to have a peak cross section of 0.2 mb and, in agreement with this result, no such processes were predicted by the computations with the limited numbers of cascades investigated.

some of these reactions are shifted substantially in energy, some others reproduce experimental data moderately well. At any rate, the magnitudes of the calculated cross sections are not far below the experimental data; this behavior would not be expected if direct interactions were primarily responsible for these reactions. The present work does not give conclusive evidence about the mechanism of $(\alpha,\alpha'\cdots)$ reactions.

IV. PARTICLE EMISSION CROSS SECTIONS

In addition to the formation cross sections of residual nuclei, it may be of interest to indicate some of the other results of the present calculations although they cannot be directly compared with existing experimental data. Table IX lists the cross sections for production of neutrons, protons, deuterons, tritons, He^3, and He^4 from various compound nuclei at 30- and 40-Mev excitation, as calculated with the DFF δ set. In addition to reflecting some of the systematic trends already noted in reference 1, the data of Table IX show that

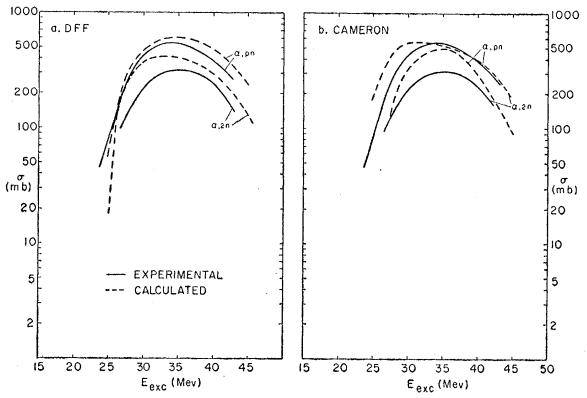

FIG. 24. Experimental[12] and calculated excitation functions for reactions of Ge^{70} with α particles (compound nucleus Se^{74}).

deuteron and alpha emission is appreciable, although always small compared with neutron and proton evaporation. Examination of the computed evaporation paths shows that, as might be expected, most of the heavy particles are emitted in the first evaporation step, at least at excitation energies up to 40 Mev. It is also worth noting that the "*pn*" products are largely formed by *pn* or *np* emission and not by deuteron evaporation. At 30-Mev excitation the proportion of these products formed by deuteron emission is of the order of 5% and at 40 Mev of the order of 10%.

V. DISCUSSION OF δ VALUES

In considering the DFF δ set (Table VII), it should be borne in mind that shell effects on level densities have been treated in the same manner as pairing effects. The values in columns 3 and 5 of Table VII thus include pairing and shell effects, whereas Cameron's δ's (columns 2 and 4) represent pairing energies only. It is

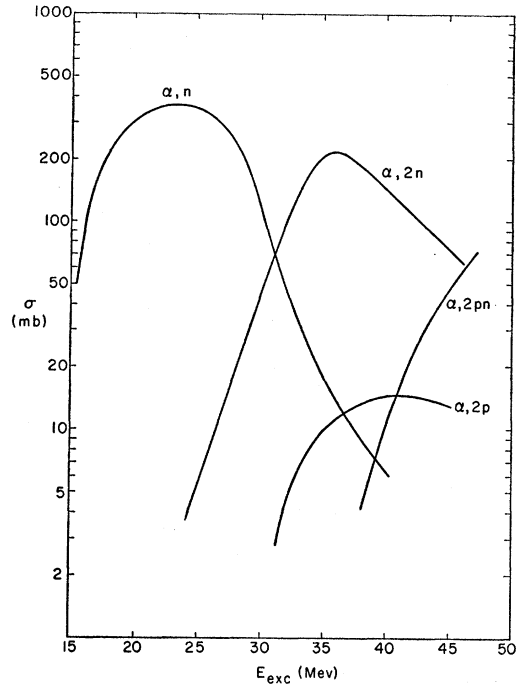

FIG. 25. Predicted excitation functions for the reaction of Sc^{45} with α particles (compound nucleus V^{49}).

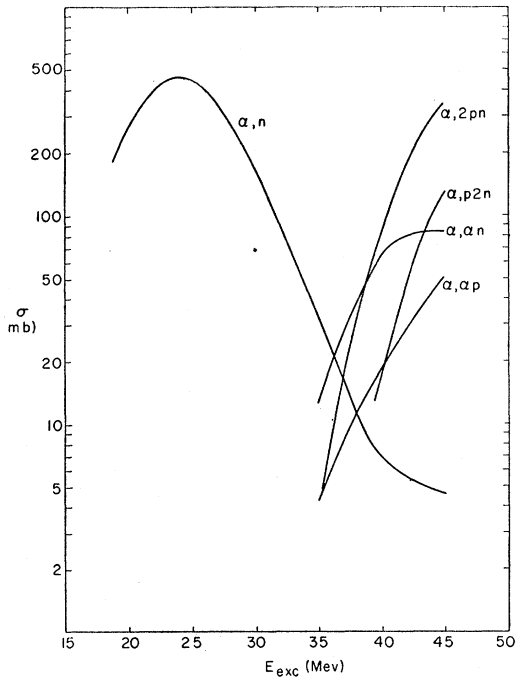

FIG. 26. Predicted excitation functions for the reaction of Cr^{50} with α particles (compound nucleus Fe^{54}).

seen that, as expected, the highest δ values in the DFF set occur at $Z=28$ and $N=28$. The low values at $Z=30$ and $N=30$ may also be attributable to the preceding shell edges. The other deviations of the DFF set of δ's from that of Cameron are all in such a direction as to repress neutron emission and favor proton emission in those reactions which were used in the fitting procedure. The necessity for this particular direction in the adjustment of the δ's may reflect a consistent overestimate of Γ_n/Γ_p with the equations and parameters used. With these equations and parameters, the DFF set of δ's appears to be moderately adequate; however, with a different choice, for example, of the value of r_0 ($>1.5\times10^{-13}$ cm), another set of δ's closer to Cameron's pairing energies might well give a good fit to experimental data. A further indication that larger interaction radii for charged particles are needed comes from the observation already mentioned that continuum theory with $r_0=1.5\times10^{-13}$ cm and $\rho_\alpha=1.2\times10^{-13}$ cm (see Eq. 4) appears to underestimate α-particle capture cross sections.[45]

After the DFF δ set had been chosen, the effect of a on the excitation functions was re-examined for the four compound nuclei Ge^{68}, Ga^{69}, Ni^{58}, and Cr^{50}, for which a large number of cross-section data were avail-

TABLE IX. Calculated cross sections (in mb) for the formation of various particles from different compound nuclei. (Calculated with DFF δ set of Table VII.)

Compound nucleus	30-Mev excitation						40-Mev excitation					
	n	p	d	t	He^3	He^4	n	p	d	t	He^3	He^4
Cr^{50}	740	690	25	0	0	49	940	1020	116	2	2	130
Mn^{54}	1300	330	14	0	0	29	1650	680	52	5	2	140
Fe^{54}	780	680	14	0	0	36	1020	1070	60	0	2	91
Ni^{58}	570	1100	19	0	0	36	860	1470	72	0	0	100
Zn^{62}	860	920	19	0	0	91	1210	1170	43	12	7	250
Zn^{64}	1270	640	25	0	0	21	1850	800	76	5	2	81
Zn^{66}	1710	290	8	2	0	21	2430	500	62	2	2	72
Ga^{67}	1190	760	28	0	0	77	1850	1000	98	10	0	160
Ga^{69}	1790	170	21	9	0	100	2490	520	55	30	0	190
Ge^{68}	730	1070	30	0	0	170	1220	1280	73	8	8	340
Ge^{74}	1870	39	2	0	0	21	3190	112	20	2	2	100
Se^{74}	1300	500	16	0	0	68	2120	780	69	2	0	180

[45] *Note added in proof.*—Additional support for a larger r_0 comes from the work of J. M. C. Scott [Phil. Mag. **45**, 441 (1954)] and J. A. Evans [Proc. Phys. Soc. (London) **73**, 33 (1959)] who showed that the Coulomb barrier around a nucleus with diffuse edge and of the shape derived from the Stanford electron scattering data can be approximated by the barrier around a uniform-density nucleus with $r_0=1.65\times10^{-13}$ cm. To test the effect of a larger r_0, most of the calculations of excitation functions presented in this paper have now been repeated with $r_0=1.70\times10^{-13}$ cm. The corresponding parameters in Eq. (2) are $\alpha=0.76+1.93A^{-\frac{1}{3}}$ and $\beta=(1.66A^{-\frac{2}{3}}-0.050)/(0.76+1.93A^{-\frac{1}{3}})$, and the parameters in Table II must be replaced by those in the following table (with $c_\alpha=0$ at all values of Z, and the relationship between the values of c and k for deuterons, tritons, and He^3 and those for protons and α particles the same as for $r_0=1.5\times10^{-13}$ cm):

Z	k_p	c_p	k_α
20	0.51	0.00	0.81
30	0.60	−0.06	0.85
40	0.66	−0.10	0.89
50	0.68	−0.10	0.93

For comparison with experiments, the capture cross sections were, of course, also recalculated with $r_0=1.70\times10^{-13}$ cm. With Cameron's δ values and this new choice of r_0, the agreement with experiment was found to be substantially better than for $r_0=1.50\times10^{-13}$ cm and in many cases about as good as for the DFF δ set and $r_0=1.50\times10^{-13}$ cm. Thus, useful calculations of excitation functions may be made with $r_0=1.70\times10^{-13}$ cm and Cameron's δ values in regions for which no adjusted δ values are available.

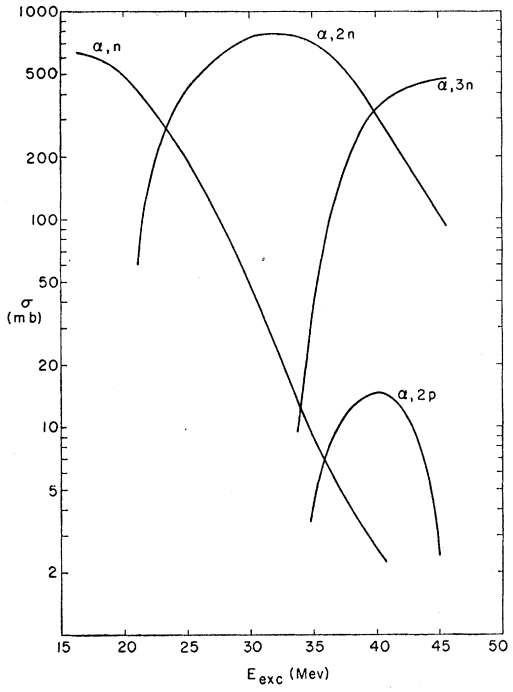

FIG. 27. Predicted excitation functions for the reaction of Co^{59} with α particles (compound nucleus Cu^{63}).

able. Although, as expected, the slopes of most excitation functions are slightly less steep with $a=A/30$ than with $a=A/20$ the differences in calculated ratios and shapes were found to be small. The earlier conclusion that the choice of a δ set is not very sensitive to the value of a is thus confirmed. No firm conclusion about a best value of A/a could be reached.

VI. SUGGESTIONS FOR FURTHER EXPERIMENTS

In Figs. 25–30 additional excitation functions are presented for reactions which are observable by activation techniques in the mass range under discussion, but for which no experimental data are available. By analogy with the data for which comparisons with experiment have been made, it may be expected that some of these curves are shifted in energy, although the shapes and the ratios of maxima should be rather reliable.

More useful even than experimental checks of cross sections predicted in this paper would be experiments designed to simplify the investigation of suitable δ choices in this and other regions of the periodic table. Following are suggestions for such experiments.

The use of experimental data on the ratio of neutron emission to proton emission from even-mass compound nuclei at low-excitation energies for the construction of loci of δ pairs was already mentioned in Sec. IIIc. From the ratio of neutron emission to proton emission from an odd-mass compound nucleus, the sum of two δ values can similarly be obtained; this determines a line of slope -1 in the plane of the two δ's. If both types of loci are available for the same pair of δ's, it should be possible to determine the two δ values uniquely from the intersection of the two lines. For example, the ratio of the $_{30}Zn^{64}(\alpha,n)_{32}Ge^{67}$ to the

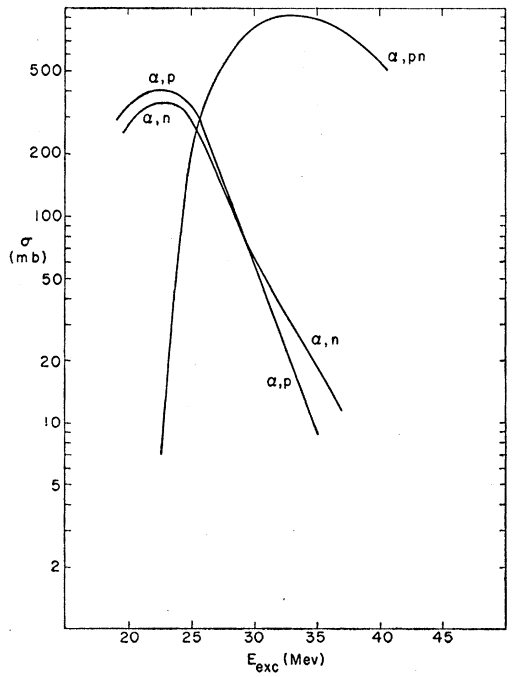

FIG. 28. Predicted excitation functions for the reaction of Ni^{58} with α particles (compound nucleus Zn^{62}).

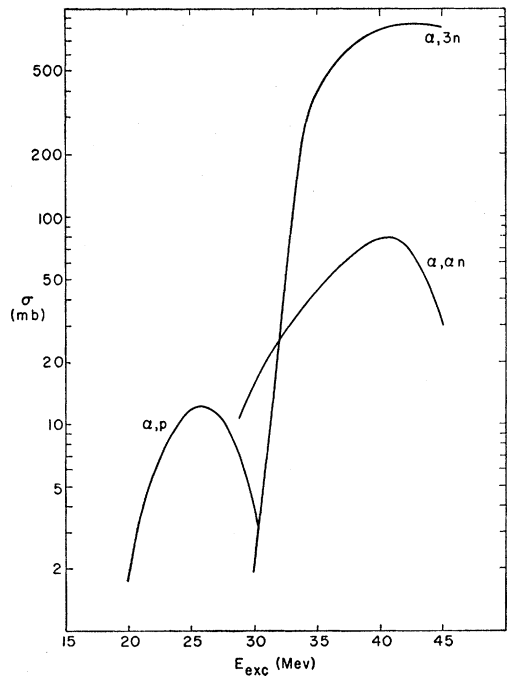

FIG. 29. Predicted excitation functions for the reaction of Zn^{70} with α particles (compound nucleus Ge^{74}).

$_{30}Zn^{64}(\alpha,p)_{31}Ga^{67}$ cross sections at about 15-Mev α energy (or 20-Mev excitation of the Ge^{68} compound nucleus) determines the relative values of δ_{Z32} and δ_{N36} (Fig. 6). From the cross sections of the reactions $_{30}Zn^{66}(He^3,n)_{32}Ge^{68}$ and $_{30}Zn^{66}(He^3,p)_{31}Ga^{68}$ the sum of δ_{Z32} and δ_{N36} can be deduced, since proton emission leads to the odd-odd nucleus Ga^{68} (for which $\delta=0$) whereas the formation of the product of neutron emission, $_{32}Ge^{68}$, is controlled by the sum of these two δ's. Thus, from these two experiments, δ_{Z32} and δ_{N36} can be determined uniquely, under the assumption, of course, that all four reactions involved proceed via compound nucleus formation.[46] A similar procedure is possible for the pairs δ_{Z30}, δ_{N32} (with He^4- and He^3-induced reactions on Ni isotopes), δ_{Z36}, δ_{N42} (with similar reactions on Se isotopes), and δ_{Z36}, δ_{N48} (also with Se reactions). The last two sets of reactions require mass spectrometric detection techniques for Kr products.

Having determined one pair of δ's in this manner, one can use them, together with other loci determined from experiments, to establish other δ values. For example, from the reactions $_{30}Zn^{64}(He^3,n)_{32}Ge^{66}$ and $_{30}Zn^{64}(He^3,p)_{31}Ga^{66}$, the sum of δ_{Z32} and δ_{N34} can be fixed, and if δ_{Z32} is now known from the previous set of experiments, this determines δ_{N34}. This procedure can

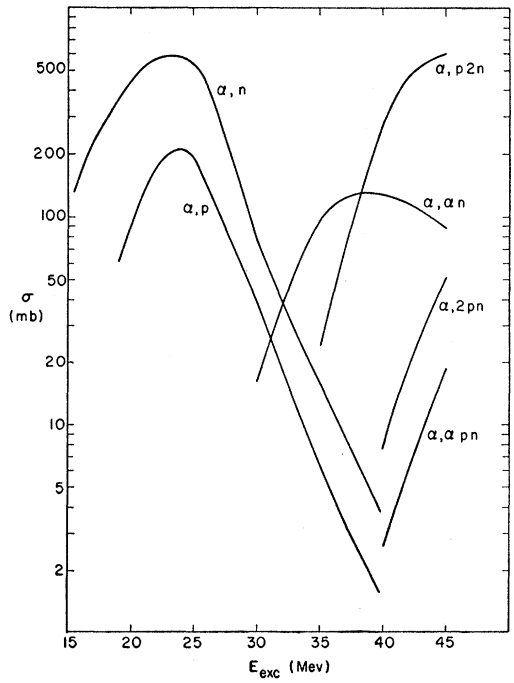

FIG. 30. Predicted excitation functions for the reaction of Ge^{70} with α particles (compound nucleus Se^{74}).

[46] For the He^3-induced reactions this assumption will certainly require confirmation. In addition, the rather large positive Q-values for the He^3 reactions make it necessary to use the lowest He^3 energies compatible with barrier considerations in order to stay below the threshold for two-nucleon emission.

TABLE X. Reactions suitable for determination of δ values.

Reactions	δ pairs for which locus can be determined	δ's whose sum can be obtained
$Ti^{46}(He^3,n)Cr^{48}$ $Ti^{46}(He^3,p)V^{48}$		$Z24$, $N24$[a]
$Ti^{46}(\alpha,n)Cr^{49}$ $Ti^{46}(\alpha,p)V^{49}$	$Z24$, $N26$	
$Cr^{50}(He^3,n)Fe^{52}$ $Cr^{50}(He^3,p)Mn^{52}$		$Z26$, $N26$[a]
$Cr^{50}(\alpha,n)Fe^{53}$ $Cr^{50}(\alpha,p)Mn^{53}$ [b]	$Z26$, $N28$	
$Fe^{54}(He^3,n)Ni^{56}$ $Fe^{54}(He^3,p)Co^{56}$		$Z28$, $N28$[a]
$Fe^{54}(\alpha,n)Ni^{57}$ $Fe^{54}(\alpha,p)Co^{57}$	$Z28$, $N30$	
$Ni^{58}(He^3,n)Zn^{60}$ $Ni^{58}(He^3,p)Cu^{60}$		$Z30$, $N30$[a]
$Ni^{58}(\alpha,n)Zn^{61}$ $Ni^{58}(\alpha,p)Cu^{61}$	**Z30, N32**[c]	
$Ni^{60}(He^3,n)Zn^{62}$ $Ni^{60}(He^3,p)Cu^{62}$		**Z30, N32**[c]
$Cu^{63}(He^3,n)Ga^{65}$ $Cu^{63}(He^3,p)Zn^{65}$	$Z30$, $N34$	
$Zn^{64}(He^3,n)Ge^{66}$ $Zn^{64}(He^3,p)Ga^{66}$		$Z32$, $N34$
$Zn^{66}(He^3,n)Ge^{68}$ $Zn^{66}(He^3,p)Ga^{68}$		**Z32, N36**[c]
$Zn^{64}(\alpha,n)Ge^{67}$ $Zn^{64}(\alpha,p)Ga^{67}$	**Z32, N36**[c]	
$Ga^{69}(He^3,n)As^{71}$ $Ga^{69}(He^3,p)Ge^{71}$	$Z32$, $N38$	
$Ge^{70}(He^3,n)Se^{72}$ $Ge^{70}(He^3,p)As^{72}$		$Z34$, $N38$
$Ge^{70}(\alpha,n)Se^{73}$ $Ge^{70}(\alpha,p)As^{73}$	$Z34$, $N40$	
$Ge^{76}(\alpha,n)Se^{79}$ $Ge^{76}(\alpha,p)As^{79}$	$Z34$, $N46$	
$Se^{74}(He^3,n)Kr^{76}$ $Se^{74}(He^3,p)Br^{76}$		$Z36$, $N40$
$Se^{74}(\alpha,n)Kr^{77}$ $Se^{74}(\alpha,p)Br^{77}$	**Z36, N42**[c]	
$Se^{76}(He^3,n)Kr^{78}$ [d] $Se^{76}(He^3,p)Br^{78}$		**Z36, N42**[c]
$Se^{77}(\alpha,n)Kr^{80}$ [d] $Se^{77}(\alpha,p)Br^{80}$		$Z36$, $N44$
$Se^{80}(He^3,n)Kr^{82}$ [d] $Se^{80}(He^3,p)Br^{82}$		$Z36$, $N46$
$Se^{80}(\alpha,n)Kr^{83}$ [d] $Se^{80}(\alpha,p)Br^{83}$	**Z36, N48**[c]	
$Se^{82}(He^3,n)Kr^{84}$ [d] $Se^{82}(He^3,p)Br^{84}$		**Z36, N48**[c]
$Se^{82}(\alpha,n)Kr^{85}$ $Se^{82}(\alpha,p)Br^{85}$	$Z36$, $N50$	

[a] These δ sums include any symmetry correction that may apply to these nuclei.
[b] The yield of the very long-lived Mn^{53} can probably be measured with mass-spectrometric techniques only.
[c] The δ pairs shown in boldface can be uniquely fixed by determination of both their sums and their loci.
[d] Stable krypton isotope, probably measurable by mass spectrometry.

be extended in an obvious way to cover most of the δ's required in any given region. Table X lists a number of reactions which can be used to determine the δ's in the region covered in the present paper. It may be noted that, as a result of various interconnections of δ values, the set is overdetermined and a number of checks are thus available. It would certainly be interesting to see if a consistent set of δ's exists.

In conclusion, it is perhaps worthwhile to restate that there is no intention to claim that a set of δ values has been derived which is unique or which gives the best fit to experimental data. Rather, the main point of the present work is to show that, with the formalism of the statistical theory, it is possible to account rather well for a large body of experimental data on excitation functions, provided level densities for any given nucleus are based on a characteristic level determined uniquely by the neutron and proton numbers in that nucleus.

ACKNOWLEDGMENTS

This work was carried out while one of the authors (G. F.) was a guest at the Weizmann Institute of Science. He wishes to express his gratitude for the hospitality extended to him. We wish to thank Professor C. L. Pekeris for his cooperation in providing time on the WEIZAC and the operating crew of the computer for their assistance. The help of Dr. P. Rabinowitz in the early phases of the programming and in providing valuable suggestions is gratefully acknowledged. Numerous stimulating discussions with Professor J. M. Miller have been particularly helpful, as has been his communication to us of unpublished experimental data. We also wish to thank Dr. N. T. Porile and Dr. S. Amiel for making their results available to us prior to publication. The assistance of Mrs. Miriam Berko and Mrs. Shulamit Rothschild in calculating and tabulating data is gratefully acknowledged.